Compositional Dependence of the Elastic Wave Velocities of Mantle Minerals: Implications for Seismic Properties of Mantle Rocks

Sergio Speziale

Department of Earth and Planetary Science, University of California, Berkeley, California

Fuming Jiang and Thomas S. Duffy

Department of Geosciences, Princeton University, Princeton, New Jersey

Using single-crystal elasticity data we constrain the effect of chemical substitutions on the elastic properties of mantle minerals and estimate the consequences for the seismic properties of mantle rocks. At ambient conditions the calculated relative variation of compressional and shear velocities $\partial \ln v_P / \partial X_{Fe}$ and $\partial \ln v_S / \partial X_{Fe}$ due to Fe–Mg substitution, range between -0.05 and -0.46 and between -0.08 and -0.74 respectively in the main mantle minerals. The corresponding heterogeneity ratios $R = \partial \ln v_S / \partial \ln v_P$ for Fe–Mg substitution range between 0.9 and 1.7 suggesting that the effect of this substitution is very different in different solid solutions systems. More limited experimental results for Ca–Mg substitution and Al enrichment in pyroxenes and garnets were also evaluated. Only Ca–Mg substitution in garnets is found to produce large (>2.0) values of R. Heterogeneity parameters at upper mantle and transition zone conditions can be substantially different from ambient P-T values in some cases. Using a first-order approximation of the effect of Fe–Mg substitution on the elastic properties of the most relevant upper mantle rocks, we find that the sensitivities of seismic velocities to Fe enrichment can vary as much as 2–3 times between the different rock types. We estimate that in the upper mantle the value of $\partial \ln v_S / \partial \ln v_P$ for pyrolite, piclogite and harzburgite decreases from 1.5 to 1.0 at the base of the transition zone, while it only decreases from 1.5 to 1.3 in mid ocean ridge basalt eclogite, which is enriched in garnet. We also estimate that the seismic effect of lateral changes in lithology from average mantle to subducted slab rocks decreases in intensity at upper mantle and transition zone depths, in agreement with seismic tomographic models. Information about the effects of Ca and Al enrichment are still too incomplete to make predictions of their effects on whole rocks, but they could be relevant based on our limited information.

1. INTRODUCTION

Earth's Deep Mantle: Structure, Composition, and Evolution
Geophysical Monograph Series 160

10.1029/160GM18

The improvement of seismological models of the Earth mantle in recent years [e.g. *Kennett et al.*, 1998; *Masters et al.*, 2000; *Gung et al.*, 2003] has focused attention to the

interpretation of a new level of details. The understanding of deviations from the radially averaged reference model requires more complete knowledge of the mechanical behavior of minerals at the conditions of the Earth interior. The majority of the heterogeneity present in global seismic tomography models can be interpreted as the effect of the thermal structure of the mantle [e.g. *Grand et al.*, 1997; *Antolik et al.*, 2003]. This interpretation has been confirmed by combined inversions of seismic and geodynamic data related to mantle flow [*Forte and Mitrovica*, 2001]. The presence of large compositional heterogeneities has been advocated based on the low correlation or anticorrelation of anomalies of bulk and shear seismic velocities at about 100 km depth and in the deepest part of the lower mantle [*Forte and Woodward*, 1997; *van der Hilst and Kárason*, 1999].

Enrichment and depletion in the average Fe content of lithospheric rocks is invoked as a mechanism of compositional stabilization of the thermal heterogeneity between the uppermost subcontinental and suboceanic mantle [*Jordan*, 1978]. This hypothesis is both supported by the available geochemical sampling of the mantle, represented by xenoliths [*Jordan*, 1979; *Lee*, 2003], and fits to geodynamical constraints [*Forte and Perry*, 2000]. The various interpretations ultimately depend on the correlation between seismic velocity anomalies and density or temperature derived from mineral physics [e.g. *Karato*, 1993; *Karato and Karki*, 2001] thereby stimulating a need for both improvement of the resolving power of tomographic models and a parallel development of a larger and more consistent base of data from mineral physics.

A major effort has been devoted to the development of in-situ high-pressure and high-temperature measurements of the thermoelastic properties of mantle minerals [*Zha et al.*, 2000; *Sinogeikin et al.*, 2004]. However, in spite of the technical advancement in high-pressure mineral physics, the basic question of the effects of compositional variations, high pressure, and high temperature on the elastic properties of the relevant minerals of the mantle has not yet been addressed comprehensively. Indeed the main components of mantle rocks are all solid solutions, often complex mixtures of three or more endmembers, and the effect of mixing is not fully taken into account in the extant mineralogical models [*Duffy and Anderson*, 1989; *Vacher et al.*, 1998; *Cammarano et al.*, 2003].

In this chapter we will evaluate the effect of composition on the elastic properties of upper mantle minerals and model rocks using an elasticity dataset derived solely from single-crystal experimental techniques. We will first calculate the sensitivity of sound wave velocities in olivine and aluminum-bearing garnets to Fe–Mg and Ca–Mg substitutions by combining new experimental results by Brillouin spectroscopy [*Jiang et al.*, 2004a, 2004b; *Speziale et al.*, 2004] with extant data. We will then extend our calculation to the effect of Fe–Mg substitution, and where possible that of Al or hydrogen incorporation, in different families of minerals of the upper mantle. We will finally estimate the effect of Fe–Mg substitution in the rocks of the upper mantle. Our results give a picture of the strengths and the limitations of the currently available single-crystal experimental data on the elastic properties of mantle minerals. The inconsistency between our estimations and the results of other studies highlights the importance of a reasoned and consistent choice of the database to be used in constructing a mineralogical model of the Earth's mantle.

2. METHODS

2.1. Elasticity Dataset

We use an elasticity dataset based on a large number of experimental results from single-crystal techniques (e.g. Brillouin scattering, impulsive stimulated scattering, resonant ultrasound spectroscopy, GHz ultrasonic interferometry) in order to place constraints on the effects of Fe–Mg substitution in different families of mantle minerals. Single-crystal elasticity measurements allow us to determine the whole elastic tensor which completely defines the elastic anisotropy, gives information about interatomic interactions and integrates the information from crystallography. In selecting the database of elastic moduli, we systematically prefer single-crystal results with respect to measurements on polycrystalline samples (e.g. by ultrasonic techniques), because of potential grain size inhomogeneity, texture effects and porosity in the polycrystalline samples that can affect the validity of these results. Direct results from elasticity measurements are also emphasized over indirect determination of bulk moduli and their pressure derivatives from high-pressure x-ray diffraction because the latter are the results of fitting experimentally measured volumes to a pressure-volume equation of state, and can be affected by significant correlation [e.g. *Angel*, 2000].

2.2. Olivine and Ternary Garnets

We compute the sensitivity of the aggregate acoustic velocities to Fe–Mg substitution in olivine, $(Mg,Fe)_2SiO_4$ as well as the sensitivity to Fe–Ca–Mg substitutions in ternary garnets in the subsystem pyrope ($Mg_3Al_2Si_3O_{12}$), almandine ($Fe_3Al_2Si_3O_{12}$), grossular ($Ca_3Al_2Si_3O_{12}$), at upper mantle conditions. By combining our new single-crystal high-pressure Brillouin spectroscopy results for

fayalite (Fe_2SiO_4) [*Speziale et al.*, 2004] and for three garnet compositions [*Jiang et al.*, 2004a, 2004b] with extant data for Mg-rich olivine [*Zha et al.*, 1996, 1998; *Abramson et al.*, 1997] and pyrope [*Sinogeikin and Bass*, 2000], we have a large coverage of the effect of chemical variation on the full elastic tensor up to upper mantle pressures for both systems.

We first derive the endmember properties of olivine by averaging available data (Table 1). In the case of ternary aluminum garnets in the subsystem $(Mg,Fe,Ca)_3Al_2Si_3O_{12}$ we proceeded by least square fitting of the large dataset of natural and synthetic garnets available in the literature. We extracted a complete set of properties for pyrope ($Mg_3Al_2Si_3O_{12}$), almandine ($Fe_3Al_2Si3O_{12}$), and grossular ($Ca_3Al_2Si3O_{12}$) reported in Table 2.

We generate mixture densities for olivine by averaging endmember densities using molar fractions as weighting factors. In the case of the ternary garnet (here treated as a mixture with complete disordered distribution of Fe, Mg, and Ca in the dodecahedral site) the densities are calculated using a regular solution model for volume mixing [*Geiger*, 1999]. We calculate thermal expansion coefficient, bulk and shear moduli, and their pressure and temperature derivatives by linear combination of the endmember properties using their molar fractions as weighting coefficients. We apply a linear mixing model because the available experimental data, both for natural and synthetic materials, do not show well resolved non-linearities.

We then compute acoustic velocities and densities of mixtures with arbitrary compositions along adiabatic pressure-temperatures paths with foot temperature of 1673 K, compatible with model geotherms for a radially averaged mantle. The zero-pressure density, bulk and shear modulus and pressure derivatives of the mixtures at 1673 K are calculated following the procedure outlined by *Duffy and Anderson* [1989]. Aggregate bulk and shear moduli along the adiabatic profiles are calculated with third order Eulerian finite strain equations [*Davies and Dziewonski*, 1975; *Duffy*

Table 1. Thermoelastic Parameters Used in the Computations of Seismic Velocity of Olivine Mixtures.

Parameter	Forsterite	Fayalite
A) ρ_0 (Mg/m^3)	3.222 (7)	4.388 (9)
B) K_S (GPa)	128.7 (5)	137.6 (3)
C) $(\partial K_S/\partial P)_T$	4.2 (2)	4.85 (5)
D) G (GPa)	81.6 (3)	51.2 (2)
E) $(\partial G/\partial P)_T$	1.6 (2)	1.8 (1)
F) $\partial^2 G/\partial P^2$ (GPa^{-1})	-0.021 (2)*	-0.11 (8)
G) γ_0	1.29 (2)	1.21 (3)
H) C_p (J/gK)	0.84	0.67
I) $\partial K_S/\partial T$ (GPa/K)	-0.016 (1)	-0.022 (5)
J) $\partial G/\partial T$ (GPa/K)	-0.014 (1)	-0.013 (1)
K) α_1 (10^{-5} K^{-1})	2.85	2.39
L) α_2 (10^{-8} K^{-2})	1.01	1.15
M) α_3 (K)	-0.384	-0.052

Numbers in parentheses are 1 standard deviation uncertainty in the last digits.

α_1, α_2, α_3, are coefficients to calculate the thermal expansion coefficient: $\alpha(T) = \alpha_1 + \alpha_2 T + \alpha_3/T^2$, where T is expressed in K.

* Required by truncation of the third-order Eulerian strain expansion.

References—Forsterite: A) *Anderson and Isaak* [1995]; B) *Isaak et al.* [1989], *Zha et al.* [1996]; C) *Zha et al.* [1996]; D) *Isaak et al.* [1989], *Zha et al.* [1996]; E) *Zha et al.* [1996]; F) calculated to be consistent with a third-order Eulerian strain fit; G) *Anderson and Isaak* [1995]; H) *Anderson and Isaak* [1995]; I) *Sumino et al.* [1977], *Isaak et al.* [1989]; J) *Sumino et al.* [1977], *Isaak et al.* [1989]; K–M) *Fei* [1995].

Fayalite : A–F) *Speziale et al.* [2004]; G–H) *Anderson and Isaak* [1995]; I) *Isaak et al.* [1993]; J) *Isaak et al.* [1993]; K–M) *Fei* [1995].

Table 2. Thermoelastic Parameters Used in the Computations of Seismic Velocity of Garnet Mixtures

Parameter	Pyrope	Almandine	Grossular
A) ρ_0 (Mg/m^3)	3.565 (1)	4.312(2)	3.600 (1)
B) K_S (GPa)*	171 (3)	175 (2)	168 (1)
C) $(\partial K_S/\partial P)_T$*	4.1 (3)	4.9 (4)	3.9 (2)
D) G (GPa)*	94 (2)	96 (2)	109 (4)
E) $(\partial G/\partial P)_T$*	1.3 (2)	1.4 (1)	1.1 (1)
F) γ_0	1.16 (9)	0.90 (9)	1.04 (9)
G) C_p (J/gK)	0.814	0.714	0.736
H) $\partial K_S/\partial T$ (GPa/K)*	-0.021 (2)	-0.022(2)	-0.015 (1)
I) $\partial G/\partial T$ (GPa/K)*	-0.008 (1)	-0.012(1)	-0.013 (1)
J) α_1 (10^{-5} K^{-1})	2.30	1.78	1.95
K) α_2 (10^{-8} K^{-2})	0.596	1.24	0.809
L) α_3 (K)	-0.454	-0.507	-0.497

α_1, α_2, α_3: as in Table 1.

*The endmember values were determined by least-square fitting of the available single-crystal data for natural mixtures.

References—Pyrope: A) *Armbruster et al.* [1992]; B) *O'Neill et al.* [1991], *Sinogeikin and Bass* [2000]; C) *Sinogeikin and Bass* [2000]; D) *Isaak and Graham* [1976], *O'Neill et al.* [1991], *Sinogeikin and Bass* [2000]; E) *Sinogeikin and Bass* [2000]; F–G) *Watanabe* [1982]; H–I) *Suzuki and Anderson* [1983], *Isaak et al.* [1992]; J–L) *Skinner* [1956].

Almandine: A) *Armbruster et al.* [1992]; B) *Isaak and Graham* [1976], *Babuška et al.* [1978], *Jiang et al.* [2004b]; C) *Jiang et al.* [2004b]; D) *Isaak and Graham* [1976], *Babuška et al.* [1978], *Jiang et al.* [2004b]; E) *Jiang et al.* [2004b]; F–G) *Watanabe* [1982]; H–I) *Isaak and Graham* [1976], *Sumino and Nishizawa* [1978]; J–L) *Skinner* [1956].

Grossular: A) *Novack and Gibbs* [1971]; B) *Bass* [1986], *O'Neill et al.* [1989], *Isaak et al.* [1992], *Chai et al.* [1997]; *Jiang et al.* [2004b]; C) *Jiang et al.* [2004b]; D) *Bass* [1986], *O'Neill et al.* [1989], *Isaak et al.* [1992]; *Chai et al.* [1997]; *Jiang et al.* [2004b]; E) *Jiang et al.* [2004b]; F-G) *Anderson and Isaak* [1995]; H-I) *Suzuki and Anderson* [1983], *Isaak et al.* [1992]; J-L) *Skinner* [1956].

and Anderson, 1989] except for the case of olivine where we use fourth order Eulerian strain equations (Table 1) because of the non-linear pressure dependence of the shear modulus G observed in fayalite [*Speziale et al.*, 2004]. We investigate selected paths in the compositional space of ternary garnets all intersecting at the "standard" composition for mantle garnets, which is 72 mol% pyrope, 14 mol% almandine, 14 mol% grossular [e.g. *McDonough and Rudnick*, 1998; *Lee*, 2003]. The results of the calculations are reported in Tables 3 and 4.

2.3. Other Mineral Families

In accordance with the philosophy of this study, we also use a dataset based on single-crystal elasticity data for other mantle mineral families. We limit our attention to ambient conditions because the single-crystal elastiticy data at high pressure or high temperature available for these systems are largely incomplete. We calculate the sensitivities of aggregate acoustic velocity to Fe–Mg exchange in orthopyroxens, clinopyroxenes of the diopside-hedenbergite series, periclase-wüstite, and in the high-pressure β- and γ- polymorphs of olivine. We determine the sensitivity of acoustic velocity to Al(Fe,Mg) substitution in orthopyroxenes and in majoritic garnets. We also estimate the effect of incorporation of water in different systems relevant for the Earth's upper mantle. The calculated sensitivities are reported in Tables 5 and 6.

2.4. Average Sensitivities of Mantle Rocks

We compute the effect Fe to Mg substitution on the seismic heterogeneity parameters in four relevant mantle rock types: pyrolite [*Ringwood*, 1975], piclogite [*Bass and Anderson*, 1984], harzburgite, and mid-ocean ridge basalt eclogite (MORB eclogite), along an isentropic pressure temperature path with a starting temperature of 1673 K. At each pressure, the bounds on the average rock heterogeneity parameters are calculated as an average, weighted by fractional volume, of the heterogeneity parameters of the single mineral

Table 3. Compositional Effect on the Compressional Velocity Heterogeneity Parameters $\partial \ln v_P/\partial X_i$, $\partial \ln v_S/\partial X_i$, $\partial \ln v_B/\partial X_i$, and the Ratio $R = \partial \ln v_S/\partial \ln v_P$ in Olivine and Ternary Aluminum Garnets.

Variable	Olivine Fe/(Fe+Mg)	Garnet Fe/(Fe+Mg) Ca/Fe = 1	Garnet Fe/(Fe+Mg) Ca/Mg = 0.19	Garnet Ca/(Ca+Mg) Fe/Mg = 0.19	Olivine + MgO Fe/(Fe+Mg) [*K and K*, 2001]	Whole rock Fe/(Fe+Mg) [*Jordan*, 1979]
$\partial \ln v_P/\partial X_i$						
1 bar, 300 K	-0.24 (1)	-0.05 (1)	-0.09 (1)	0.03 (1)	-0.4 (1)	-0.27
1 bar, 1673 K	-0.27 (1)	-0.08 (1)	-0.11 (1)	0.03 (1)		
4 GPa (high T)	-0.25 (1)	-0.08 (1)	-0.10 (1)	0.02 (1)		
8 GPa (high T)	-0.24 (1)	-0.08 (1)	-0.10 (1)	0.02 (1)		
14 GPa (high T)	-0.24 (1)	-0.08 (1)	-0.09 (1)	0.01 (1)		
$\partial \ln v_S/\partial X_i$						
1 bar, 300 K	-0.37 (1)	-0.08 (1)	-0.08 (1)	0.08 (1)	-0.5 (1)	-0.34
1 bar, 1673 K	-0.41 (1)	-0.08 (1)	-0.12 (1)	0.05 (1)		
4 GPa (high T)	-0.39 (1)	-0.08 (1)	-0.12 (1)	0.04 (1)		
8 GPa (high T)	-0.38 (1)	-0.08 (1)	-0.12 (1)	0.03 (1)		
14 GPa (high T)	-0.40 (1)	-0.09 (1)	-0.11 (1)	0.03 (1)		
$\partial \ln v_B/\partial X_i$						
1 bar, 300 K	-0.14 (1)	-0.08 (1)	-0.08 (1)	0.00 (1)	-0.2 (1)	-0.21
1 bar, 1673 K	-0.16 (1)	-0.08 (1)	-0.10 (1)	0.02 (1)		
4 GPa (high T)	-0.15 (1)	-0.08 (1)	-0.09 (1)	0.01 (1)		
8 GPa (high T)	-0.15 (1)	-0.08 (1)	-0.08 (1)	0.01 (1)		
14 GPa (high T)	-0.15 (1)	-0.07 (1)	-0.08 (1)	0.01 (1)		
$\partial \ln v_S/\partial \ln v_P$						
1 bar, 300 K	1.54 (8)	1.6 (4)	0.9 (1)	2.7 (6)	1.3 (4)	1.3
1 bar, 1673 K	1.52 (7)	1.0 (2)	1.1 (1)	1.7 (5)		
4 GPa (high T)	1.56 (7)	1.0 (2)	1.2 (2)	2.0 (7)		
8 GPa (high T)	1.58 (8)	1.0 (2)	1.2 (2)	1.5 (7)		
14 GPa (high T)	1.67 (8)	1.1 (2)	1.2 (2)	3 (2)		

High temperature values are calculated along an adiabat with 1673 K foot temperature. K and K: *Karato and Karki* [2001].

Table 4. Logarithmic Derivative of the Compressional Velocity with Respect to Density, $\partial \ln v_P/\partial \ln \rho$, $\partial \ln v_S/\partial \ln \rho$, and $\partial \ln v_B/\partial \ln \rho$ for Compositional Variations in Olivine and Ternary Aluminum Garnets.

Variable	Olivine Fe/(Fe+Mg)	Garnet Fe/(Fe+Mg) Ca/Fe = 1	Garnet Fe/(Fe+Mg) Ca/Mg = 0.19	Garnet Ca/(Ca+Mg) Fe/Mg = 0.19	Olivine + MgO Fe/(Fe+Mg) [*K and K*, 2001]	Whole rock Fe/(Fe+Mg) [*Jordan*, 1979]
$\partial \ln v_P/\partial \ln \rho$						
1 bar, 300 K	-0.67 (5)	-0.26 (3)	-0.52 (5)	-1.6 (2)	-0.8 (4)	-0.84
1 bar, 1673 K	-0.76 (6)	-0.40 (4)	-0.63 (6)	-1.7 (2)		
4 GPa (high T)	-0.69 (7)	-0.39 (4)	-0.58 (6)	-0.9 (1)		
8 GPa (high T)	-0.67 (6)	-0.38 (4)	-0.60 (6)	-0.7 (1)		
14 GPa (high T)	-0.66 (6)	-0.38 (4)	-0.50 (6)	-0.3 (1)		
$\partial \ln v_S/\partial \ln \rho$						
1 bar, 300 K	-1.1 (1)	-0.40 (4)	-0.48 (5)	-3.7 (4)	-1.0 (4)	-1.06
1 bar, 1673 K	-1.2 (1)	-0.38 (4)	-0.69 (7)	-3.1 (3)		
4 GPa (high T)	-1.1 (1)	-0.40 (4)	-0.72 (7)	-2.0 (2)		
8 GPa (high T)	-1.1 (1)	-0.41 (4)	-0.70 (7)	-1.7 (2)		
14 GPa (high T)	-1.0 (1)	-0.43 (4)	-0.62 (7)	-2.0 (2)		
$\partial \ln v_B/\partial \ln \rho$						
1 bar, 300 K	-0.37 (4)	-0.39 (5)	-0.44 (4)	0.00 (1)	-0.4 (3)	-0.66
1 bar, 1673 K	-0.44 (4)	-0.37 (4)	-0.57 (6)	-2.3 (2)		
4 GPa (high T)	-0.41 (4)	-0.38 (4)	-0.51 (5)	-0.8 (1)		
8 GPa (high T)	-0.40 (5)	-0.37 (4)	-0.47 (5)	-0.5 (1)		
14 GPa (high T)	-0.39 (4)	-0.34 (4)	-0.48 (5)	-0.3 (1)		

High temperature values are calculated along an adiabat with 1673 K foot temperature. K and K: *Karato and Karki* [2001].

phases. The modal compositions for the different rock types are inferred from experimental and computational studies [*Irifune and Ringwood*, 1987b; *Ita and Stixrude*, 1992] and are reported in Table 7.

We approximate the pressure and temperature effects on seismic heterogeneity induced by Mg-Fe substitution in the system ringwoodite–γ-Fe_2SiO_4 by combining isobaric temperature dependence and isothermal pressure dependence of the heterogeneity parameters from the available experimental data. Due to the absence of single-crystal high-pressure data on the effect of Fe–Mg substitution in pyroxenes and β-$(Mg,Fe)_2SiO_4$, we adopt the data available for these minerals groups at ambient conditions. The sensitivity of majoritic garnet to Fe–Mg substitution is assumed to be equivalent to that of Al-garnet.

We have first tested our averaging scheme in the case of arbitrary mixtures of olivine and ternary garnets in different proportions by comparing our calculations with heterogeneity parameters calculated as the relative variation of the average of Hashin–Shtrikmann bounds [*Hashin and Shtrikman*, 1961, 1963] for the velocities of the same mixtures in response to variation of the Fe content of the two component minerals. The parameters calculated at different pressures and different minerals proportions are in agreement between the two methods, within the estimated uncertainties.

3. RESULTS AND DISCUSSION

3.1. Olivine and Ternary Aluminum Garnets

The substitution of Fe for Mg in olivine results in a strong shear modulus weakening [*Graham et al.*, 1988; *Isaak et al.*, 1993], with 37% decrease of the shear modulus G, across the solid solution, and stiffening of the bulk modulus K corresponding to 7% increase from forsterite (α-Mg_2SiO_4) to fayalite (α-Fe_2SiO_4) [*Speziale et al.*, 2004]. The pressure derivative of the bulk modulus also increases with the increase of Fe content (Table 1), and the difference between the bulk moduli of forsterite and fayalite is increased to 9% at 10 GPa [*Speziale et al.*, 2004]. The pressure derivative of the shear modulus of olivine is less sensitive to the Fe content than that of the bulk modulus (Table 1). The difference of compressional sound velocity between forsterite and fayalite is 20.2% at ambient pressure and remains 17% at the pressures consistent with the bottom of the upper mantle. The variation of shear velocity is even larger: 32.1% at ambient pressure and 26% at 13 GPa.

The compositional effect on both the shear and compressional velocities at constant pressure can be represented by velocity heterogeneity parameters (also referred as compositional heterogeneity parameters in the following discussions) expressed as $(\partial \ln v_{P,S}/\partial X_i)_P$, [*Jordan*, 1979] where V_P and V_S

Table 5. Compositional Effect on the Compressional, Shear, and Bulk Velocity Heterogeneity Parameters in Different Solid Solution Series Calculated at Ambient Conditions.

Solid solution series	X	$\partial \ln v_P/\partial X$	$\partial \ln v_S/\partial X$	$\partial \ln v_B/\partial X$	$\partial \ln v_S/\partial \ln v_P$	$\partial \ln v_P/\partial \ln \rho$	$\partial \ln v_S/\partial \ln \rho$	$\partial \ln v_B/\partial \ln \rho$
Forsterite–fayalite	Fe/(Mg+Fe)	-0.24 (1)	-0.37 (1)	-0.14 (1)	1.54 (8)	-0.67 (5)	-1.1 (1)	-0.37 (4)
Al-garnet (Ca/Mg = constant)	Fe/(Mg+Fe)	-0.09 (1)	-0.08 (1)	-0.09 (2)	0.9 (1)	-0.52 (5)	-0.48 (5)	-0.44 (4)
Al-garnet (Ca/Fe = constant)	Fe/(Mg+Fe)	-0.05 (1)	-0.08 (1)	-0.08 (1)	1.6 (3)	-0.26 (3)	-0.40 (4)	-0.39 (5)
Orthoenstatite–orthoferrosilite	Fe/(Mg+Fe)	-0.21 (2)	-0.30 (4)	-0.14 (2)	1.4 (3)	-0.92 (9)	-1.3 (3)	-0.59 (6)
Diopside–hedenbergite	Fe/(Mg+Fe)	-0.09 (1)	-0.15 (2)	-0.04 (1)	1.7 (3)	-0.79 (8)	-1.4 (1)	-0.37 (4)
Wadsleyite–β-Fe_2SiO_4	Fe/(Mg+Fe)	-0.37 (5)	-0.52 (6)	-0.23 (6)	1.4 (2)	-1.2 (2)	-1.6 (2)	-0.8 (4)
Ringwoodite–γ-Fe_2SiO_4	Fe/(Mg+Fe)	-0.18 (3)	-0.28 (4)	-0.09 (5)	1.6 (3)	-0.48 (4)	-0.74 (5)	-0.26 (5)
Periclase–wüstite	Fe/(Mg+Fe)	-0.46 (5)	-0.74 (7)	-0.27 (2)	1.6 (2)	-1.0 (1)	-1.5 (2)	-0.35 (4)
Mg,Fe-Opx–Mg-Tschermak	$Al^{VI}/(Al^{VI}+Mg+Fe)^*$	0.24 (4)	0.13 (4)	0.33 (6)	0.6 (5)	7 (2)	4 (2)	10 (4)
Majorite–pyrope	$Al/(Al+Mg^{VI}+Si^{VI})^*$	0.03 (1)	0.04 (1)	0.02 (1)	1.3 (3)	1.2 (1)	1.5 (1)	0.8 (1)
Al-garnet (Fe/Mg = constant)	Ca/(Mg+Ca)	0.03 (1)	0.08 (1)	0.00 (1)	2.7 (6)	-1.6 (2)	-3.7 (4)	0.00 (3)

*Al^{VI}, Mg^{VI}, Si^{VI} are in octahedral coordination.

References—Orthoenstatite–orthoferrosilite: *Kumazawa* [1969]; *Frisillo and Barsch* [1972]; *Weidner et al.* [1978]; *Bass and Weidner* [1984]; *Duffy and Vaughan* [1988]; *Webb and Jackson* [1993]; *Jackson et al.* [1999]. Diopside–hedenbergite: *Kandelin and Weidner* [1988]; *Collins and Brown* [1998]; *Isaak and Ohno* [2003]. Wadsleyite–β-Fe_2SiO_4: *Sawamoto et al.* [1984]; *Sinogeikin et al.* [1998]; *Zha et al.* [1998]. Ringwoodite–γ-Fe_2SiO_4: *Weidner et al.* [1984]; *Rigden and Jackson* [1991]; *Rigden et al.* [1992]; *Sinogeikin et al.* [1997]; *Jackson et al.* [2000]; *Sinogeikin et al.* [2003a]. Majorite–pyrope: *Bass and Kanzaki* [1990]; *Yeganeh-Haeri et al.* [1990]; *O'Neill et al.* [1991]; *Sinogeikin and Bass* [2000]; *Sinogeikin et al.* [2002]. Periclase–wüstite: *Sinogeikin and Bass* [2000]; *Jacobsen et al.* [2002].

are the compressional and shear velocity and X_i represents the molar fraction of Fe, X_{Fe} = Fe/(Fe + Mg). Another important parameter is the compositional heterogeneity parameter ratio $R = (\partial \ln v_S/\partial \ln v_P)_P$, defined as the ratio of $(\partial \ln v_S/\partial X_i)_P$ and $(\partial \ln v_P/\partial X_i)_P$. In order to simplify the notation, all the compositional heterogeneity parameters and ratios will be hereafter considered as defined at constant pressure unless differently specified.

Heterogeneity parameters for olivine along an adiabatic path starting at 1673 K are presented in Figure 1. Consistent with our model of linear mixing of the endmember densities and aggregate moduli, we observe that the calculated effect of Fe substitution for Mg on shear velocity of olivine is slightly sensitive to the composition of the olivine itself (inset in Figure 1). However, within uncertainty, the second order coefficient is not constrained, and we limit our analysis to the linear term. Our estimation for $\partial \ln v_P/\partial X_{Fe}$ and $\partial \ln v_S/\partial X_{Fe}$ at ambient conditions are -0.24 ± 0.01 and -0.37 ± 0.01. The compositional heterogeneity parameters ratio $R = \partial \ln v_S/\partial \ln v_P$ is 1.54 ± 0.08. Our results are only in marginal agreement with the results presented by *Karato and Karki* [2001] and in disagreement with the estimates by *Jordan* [1979] for an average peridotite. We can also resolve the effect of pressure and temperature on the compositional heterogeneity parameters. At pressure above 8 GPa, $\partial \ln v_S/\partial X_{Fe}$ reverts its trend and it starts to increase (in absolute value), while $\partial \ln v_P/\partial X_{Fe}$ becomes pressure insensitive (Figure 1). This change of behavior at depth is the consequence of the very different pressure dependencies of both bulk and shear moduli of the two endmembers. In fact it also appears at pressures above 10 GPa at ambient temperature. Metastability and incipient shear softening of the Fe-rich endmember [*Speziale et al.*, 2004] could be the explanation of the reversal. This observation emphasizes the need for direct measurements at high pressure and temperature to avoid possible complications associated with room temperature metastability. The effect on elastic velocity of density variations associated with chemical exchange is expressed by the logarithmic derivatives $\partial \ln v_{P,S}/\partial \ln \rho$. The logarithmic derivative $\partial \ln v_P/\partial \ln \rho$ and for Fe–Mg substitution in olivine is -0.67, lower but still in agreement within uncertainty with the estimation of *Karato and Karki* [2001]. The value of $\partial \ln v_S/\partial \ln \rho$ is -1.1, in excellent agreement with that reported by *Karato and Karki* [2001]. The logarithmic derivatives of compressional and shear velocity decrease 10% and 15% respectively with pressure along an adiabatic profile with foot temperature of 1673 K (Table 4).

The effect of Fe–Ca–Mg substitutions on the elastic velocities of garnets in the pyrope–almandine–grossular subsystem is more complex than the simple Fe–Mg substitution in olivine. Substitution of Fe for Mg causes as much as 8.5% and 8.2% decreases of compressional and shear velocity at ambient pressure, and 7.2% and 7.7% respectively, at 14 GPa. Substitution of Ca for Fe produces 10.2% and 14.9% increases of compressional and shear velocity at ambient pressure, and 7.3% and 12% increases at 14 GPa [*Jiang et al.*, 2004b].

In the case of ternary garnets we define two heterogeneity parameters X_{Fe} = Fe/(Fe + Mg) and X_{Ca} = Ca/(Ca + Mg) for Fe–Mg and for Ca–Fe substitutions, respectively. In addition to the heterogeneity parameter we have to specify a second ratio to completely determine the compositional path along which the heterogeneity parameter is defined. As an

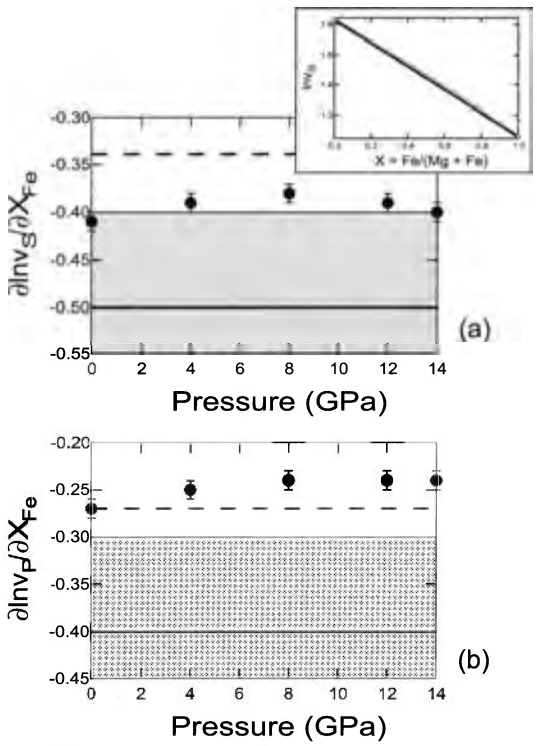

Figure 1. Compositional heterogeneity parameters of (a) shear and (b) compressional velocity for Fe–Mg substitution in olivine calculated along an adiabatic pressure / temperature path with foot temperature of 1673 K. Inset: the sensitivity of shear velocity, here plotted as $\ln v_S$, to Mg–Fe substitution calculated at ambient conditions (gray area: 1σ estimated uncertainty) suggests the existence of second order effects (see text). Dashed line: sensitivity of elastic wave velocity of lherzolite by Jordan [1979]. Continuous line: sensitivity for (Mg,Fe)O and olivine by *Karato and Karki* [2001] with uncertainty (shaded area).

example, a mixture of 70% Mg component, 10% Fe component and 20% of Ca component has the same X_{Fe} as a mixture of 77% Mg component, 11% Fe component and 12% Ca component, but it has different mixture properties because it is richer in the Ca component. In fact, the apparent effect of Fe enrichment is different in the case in which we maintain Ca/Fe = 1, compatible with the ratio for average peridotitic garnets (see section 2.2), with respect to the case in which Ca/Mg is fixed to the value 0.19 typical of average peridotitic garnets (Figure 2). The depth dependence of the heterogeneity parameters for the shear velocity ($\partial \ln v_S/\partial X_{Fe}$) along the adiabatic path have opposite sign in the two cases and the heterogeneity parameters tend to converge at pressures of the transition zone (Figure 2). The same effect can be also observed for $\partial \ln v_P/\partial X_{Fe}$.

Previous estimates of the effect of Fe to Mg substitution in an average peridotitic mineral assemblage [*Jordan*, 1979] are in substantial disagreement with the results for garnets both for shear and compressional heterogeneity parameters (Figure 2). The disagreement cannot be compensated by olivine (Figure 2a). In garnets, we observe non-linearity in the calculated sensitivity of shear velocity to the Fe–Mg substitution, as in olivine. However, the overall uncertainty associated with the calculation does not allow us to resolve this second order effect.

The logarithmic derivatives of shear and compressional elastic wave velocities with respect to density, $\partial \ln v_i/\partial \ln \rho$, for Fe to Mg substitution in garnet are systematically smaller than those for olivine (Table 4) and both are smaller than the estimates presented by *Karato and Karki* [2001]. In addition,

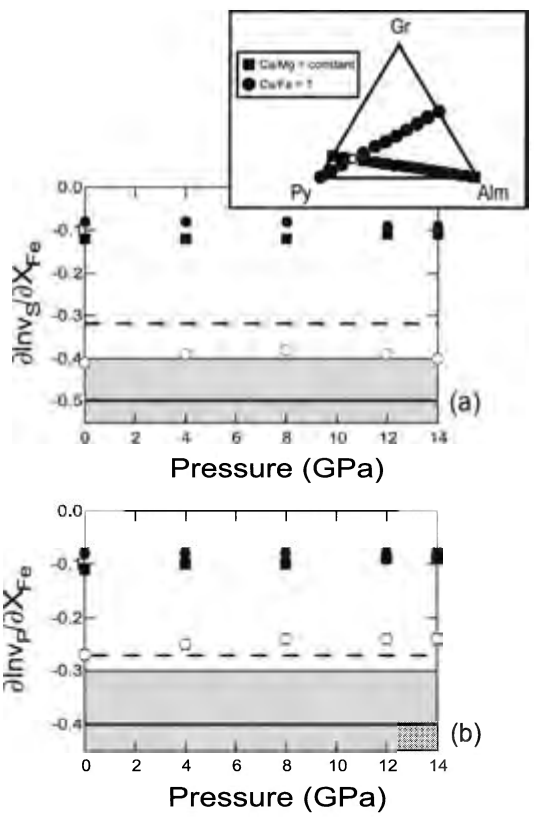

Figure 2. Compositional heterogeneity parameters of (a) shear and (b) compressional elastic wave velocity for Fe–Mg substitution in ternary aluminum-garnet in the case of Ca/Mg = constant (solid squares) and Ca/Fe = 1 (solid circles). The heterogeneity parameters are calculated along an adiabatic pressure / temperature path with foot temperature of 1673 K. Heterogeneity parameters of olivine (open circles) are reported for comparison. Dashed line: sensitivity of elastic wave velocity of lherzolite by *Jordan* [1979]. Continuous line: sensitivity for (Mg,Fe)O and olivine by *Karato and Karki* [2001] with uncertainty (shaded area). Inset: Compositional variation due to Fe–Mg substitution in ternary garnets in the cases examined in this study.

Table 6. Sensitivity of the Velocity Heterogeneity Parameters to Hydration in Different Solid Solution Series Calculated at Ambient Conditions.

Solid solution series	X	$\partial \ln v_P/\partial X$	$\partial \ln v_S/\partial X$	$\partial \ln v_B/\partial X$	$\partial \ln v_S/\partial \ln v_P$	$\partial \ln v_P/\partial \ln \rho$	$\partial \ln v_S/\partial \ln \rho$	$\partial \ln v_B/\partial \ln \rho$
Olivine humite group	$H^*/(H^*+Si)$	-0.2 (1)	-0.2 (1)	-0.2 (1)	1.0 (7)	1.7 (3)	1.1 (3)	2.2 (2)
Ringwoodite hydrous ringwoodite	$2H^*/(2H^*+Mg)$	-0.5 (1)	-0.5 (3)	-0.6 (2)	1.0 (6)	1.3 (3)	1.3 (6)	1.3 (4)
Mg,Fe-Opx–Mg-Tschermak	$H^*/(H^*+Si)$	-0.4	-0.4	-0.4	1.0	1	1	1
Periclase–wüstite brucite	$2H^*/(O-2H^*)$	-0.4	-0.5	-0.4	1.3	1	1	1

($H^* = H/4$.)

References—Olivine–humite group: *Zha et al.* [1996]; *Beckman Fritzel and Bass* [1997]; *Sinogeikin and Bass* [1999]. Ringwoodite–γ-Fe_2SiO_4: *Weidner et al.* [1984]; *Rigden et al.* [1992]; *Inoue et al.* [1998]; *Jackson et al.* [2000]; *Wang et al.* [2003]. Grossular–hydrogrossular: *Bass* [1989]; *O'Neill et al.* [1989]; *Isaak et al.* [1992]; *O'Neill et al.* [1993]; *Chai et al.* [1997]; *Jiang et al.* [2004b]. Periclase–brucite: *Xia et al.* [1998]; *Sinogeikin and Bass* [2000].

under upper mantle pressures and temperatures, our calculations show that the values of $\partial \ln v_P/\partial \ln \rho$ and $\partial \ln v_S/\partial \ln \rho$ for garnets can vary as much as 50% relative to ambient conditions. In conclusion we cannot generalize the effect of Fe–Mg substitution between these two families of minerals.

We also analyze the effect of Ca enrichment or depletion in garnets at constant Fe/Mg ratio, compatible with that of peridotitic garnets (Figure 3). The effect of pressure is to decrease the value of the heterogeneity parameters both for compressional and shear velocity. At ambient conditions, the compositional heterogeneity parameters ratio $R = \partial \ln v_S/\partial \ln v_P$, due to Ca–Mg substitution, is equal to 2.7 ± 0.6, almost 2 times larger than the ratio related to Fe–Mg substitution in olivine and in garnet. This value is also larger than R in other solid solutions systems, as we will see in the following sections. A large value of $R > 2.7$ for Ca–Mg substitution has been inferred from comparison of theoretically calculated seismic velocities in perovskites by *Karato and Karki* [2001] who suggest that Ca variation can contribute to large R values in the deep mantle. Although also not a solid solution, the comparison of seismic velocities of orthoenstatite ($MgSiO_3$) and diopside ($CaMgSi_2O_6$), based on the available data at ambient conditions [*Weidner et al.*, 1978; *Jackson et al.*, 1999; *Isaak and Ohno*, 2003], yields $R = 7 \pm 4$. The data for Ca–Mg substitution in these three systems all yield very large values of R at ambient conditions. However, our calculated value of R for Ca–Mg substitution in ternary Al-garnet averages at 1.7 ± 0.5 at upper mantle conditions and increases to 3 ± 2 in the transition zone (Table 3). A qualitative explanation of this result is that along our adiabatic path, the effect of temperature which reduces the value of R, is stronger at upper mantle depths while the effect of pressure (which increases R) becomes dominant at transition zone depths due to the shallow temperature gradient. In view of the complex combined effect of

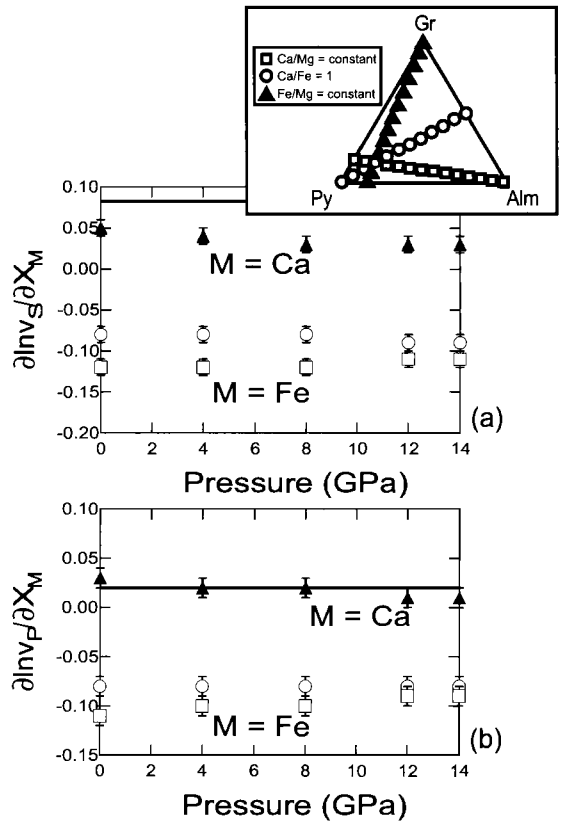

Figure 3. Compositional heterogeneity parameters of shear (a) and compressional velocity (b) for Ca–Mg substitution (solid triangles) in ternary aluminum–garnet calculated along an adiabatic pressure/temperature path with foot temperature of 1673 K. The heterogeneity parameters for Fe–Mg substitution in garnet are plotted for comparison as open symbols (cf. Figure 2). Line: sensitivity of elastic wave velocity for compositional variation between $MgSiO_3$-perovskite and $CaSiO_3$-perovskite by *Karato and Karki* [2001]. Inset: Compositional variation in ternary garnets for Ca–Fe–Mg substitutions examined in this study.

Table 7. Composition of Different Mantle Rock Types Used in Calculations.

Rock type	Bulk composition	Modal composition Mineral	(vol%)	Mineral composition Mg	Fe	Ca(mol.frac.)
Pyrolite						
SiO_2	44.31	olivine	59	0.88	0.12	
Al_2O_3	5.40	clinopyroxene	13	0.45	0.05	0.50
FeO	8.56	orthopyroxene	9	0.91	0.10	
MgO	37.82	garnet	19	0.82	0.14	0.04
CaO	3.48					
Piclogite						
SiO_2	44.69	olivine	41	0.88	0.12	
Al_2O_3	8.35	clinopyroxene	26	0.44	0.06	0.50
FeO	8.28	orthopyroxene	9	0.87	0.13	
MgO	30.24	garnet	24	0.62	0.19	0.19
CaO	8.43					
MORB eclogite						
SiO_2	47.20	olivine				
Al_2O_3	14.51	clinopyroxene	72	0.35	0.15	0.50
FeO	11.81	orthopyroxene				
MgO	12.10	garnet	28	0.45	0.35	0.25
CaO	13.19					
Harzburgite						
SiO_2	43.64	olivine	81	0.91	0.09	
Al_2O_3	0.65	clinopyroxene				
FeO	7.83	orthopyroxene	19	0.93	0.07	
MgO	46.36	garnet				
CaO	0.50*					

*Neglected in calculations. olivine $(Mg,Fe)_2SiO_4$; clinopyroxene $(Mg,Fe,Ca)_2Si_2O_6$; orthopyroxene $(Mg,Fe,Al)(Si,Al)SiO_3$; garnet $(Mg,Fe,Ca)_3Al_2Si_3O_{12}$.
References—Rock chemical and modal compositions: *Akaogi and Akimoto* [1979]; *Anderson and Bass* [1986]; *Irifune et al.* [1986]; *Irifune and Ringwood* [1987a,b, 1993]; *Ita and Stixrude* [1992, 1993]; *Irifune and Isshiki* [1998]; *Vacher et al.* [1998].

pressure and temperature, the available experimental results at ambient conditions must be used with caution in approximating the effects of Ca–Mg substitution at transition zone and lower mantle conditions.

3.2. Other Systems

The differences that we observed between the effect of Fe to Mg substitution in olivine and garnets highlight inherent risks involved in gross generalizations of compositional effects on the elastic properties of a limited subset of minerals to those of the rocks of the mantle as a whole [e.g. *Karato and Karki*, 2001]. Information about the chemical composition of the mantle should be accompanied by a precise petrological and mineralogical model. For this reason we calculate the heterogeneity parameters for Fe–Mg substitution, and where possible for other substitutions, for other minerals of the mantle based on single-crystal elasticity measurement consistent with the strategy adopted for garnet and olivine. Unfortunately, the available elastic data for the members of the different families of mantle minerals are fragmentary. For this reason we limit our calculations to ambient conditions. All the computed logarithmic derivatives of compressional and shear velocity presented for the different systems discussed in the following sections are reported in Table 5.

3.2.1. Orthopyroxene. Al-free pyroxene, $(Mg,Fe)SiO_3$, is an abundant component in mantle rocks, with a compositional range varying from 98 to 82 mol% $MgSiO_3$ [*McDonough and Rudnick*, 1998]. Different studies have been performed to determine the whole elastic tensor of different compositions in the orthoenstatite ($MgSiO_3$)–orthoferrosilite ($FeSiO_3$) solid solution series, at ambient conditions [e.g. *Webb and Jackson*, 1993; *Duffy and Vaughan*, 1988; *Jackson et al.*, 1999]. The available data are mainly limited to Mg-rich compositions with less than 10 mol% orthoferrosilite content augmented by a study of orthoferrosilite [*Bass and Weidner*,

1984]. The available data yield $\partial \ln v_P/\partial X_{Fe} = -0.21 \pm 0.02$, and $\partial \ln v_S/\partial X_{Fe} = -0.30 \pm 0.04$, which are comparable to olivine values ($\partial \ln v_P/\partial X_{Fe} = -0.24 \pm 0.01$, and $\partial \ln v_S/\partial X_{Fe} = -0.37 \pm 0.01$). However, the logarithmic derivatives of velocity with respect to density $\partial \ln v_P/\partial \ln \rho = -0.9 \pm 0.1$, and $\partial \ln v_S/\partial \ln \rho = -1.3 \pm 0.3$ are substantially different from those of olivine.

Chai et al. [1997] measured the elastic tensor of an orthorhombic pyroxene containing 2.6 weight% Al. By comparison with the calculated velocity for an Al-free orthopyroxene with the same Fe/Mg ratio, we calculate an average sensitivity of the heterogeneity parameters to Al enrichment in orthorhombic pyroxene: $\partial \ln v_P/\partial X_{Ts} = 0.24 \pm 0.04$, and $\partial \ln v_S/\partial X_{Ts} = 0.13 \pm 0.04$, where Ts = $MgAl_2SiO_6$ is the Mg-tschermak component. The presence of Al increases the acoustic velocity of orthorhombic pyroxene, in agreement with the observations for other silicate systems. The effect of Al enrichment on density is smaller than that on velocity, and the logarithmic derivatives $\partial \ln v_i/\partial \ln \rho$ are larger than unity albeit with large uncertainties (Table 5).

3.2.2. Clinopyroxene. A second pyroxene is also present in fertile lherzolites. It is a Ca-rich monoclinic member of the diopside ($MgCaSi_2O_6$)–hedenbergite ($FeCaSi_2O_6$) solid solution series. The composition of Ca-rich clinopyroxene in mantle rocks ranges between 88 and 95 mol% diopside component [*McDonough and Rudnick*, 1998].

Because of the complexity of the monoclinic elastic tensor, only a few studies of the single-crystal elasticity of Ca-rich clinopyroxenes are available in the literature [*Kandelin and Weidner*, 1988; *Collins and Brown*, 1998; *Isaak and Ohno*, 2003]. However, the extant data cover a wide range of compositons, from pure Fe-endmember to almost pure (98 mol%) Mg-endmember.

The seismic heterogeneity parameters for Ca-rich clinopyroxenes are $\partial \ln v_P/\partial X_{Fe} = -0.09 \pm 0.01$, and $\partial \ln v_S/\partial X_{Fe} = -0.15 \pm 0.02$, generally smaller than those of olivine and orthopyroxene and closer to the range of values determined for ternary aluminum garnets. On the other hand, the logarithmic derivatives of velocity with respect to density are in close agreement with those of olivine, once again showing that the relationship between compositional effect on the elastic moduli and on density is structure-specific in the different solid-solution series (Table 5).

3.2.3. β-$(Mg,Fe)_2SiO_4$ and γ-$(Mg,Fe)_2SiO_4$. Different studies of single-crystal elasticity of the high-pressure polymorphs of olivine have been published. Data for β-$(Mg,Fe)_2SiO_4$ (β-phase) are limited to Fe contents in the range 0–9 mol% [e.g. *Zha et al.*, 1998; *Sinogeikin et al.*, 1998]. The effect of Fe–Mg substitution is strong; in fact the heterogeneity parameters $\partial \ln v_P/\partial X_{Fe}$ and $\partial \ln v_S/\partial X_{Fe}$ of β-$(Mg,Fe)_2SiO_4$ are -0.37 ± 0.05 and -0.52 ± 0.06, larger than those of olivine and pyroxenes. Data for γ-$(Mg,Fe)_2SiO_4$ (γ-phase) span a larger compositional range, from pure ringwoodite (γ-Mg_2SiO_4) to γ-$(Mg_{0.75},Fe_{0.25})_2SiO_4$ [*Jackson et al.*, 2000; *Sinogeikin et al.*, 2003]. The heterogeneity parameters $\partial \ln v_P/\partial X_{Fe}$ and $\partial \ln v_S/\partial X_{Fe}$ of γ-$(Mg,Fe)_2SiO_4$ are -0.18 ± 0.03 and -0.28 ± 0.04. They are closer to olivine than those of β-phase (Table 5). However, because of the limited coverage of the compositional variation in the system β-$(Mg,Fe)_2SiO_4$, this result should be considered with caution.

3.2.4. Majorite–pyrope mixture. Due to the high abundance of garnet–majorite solid solution in the transition zone in mineralogical models of the mantle [*Ringwood*, 1975; *Duffy and Anderson*, 1989], the binary solution series between majorite ($Mg_4Si_4O_{12}$) and pyrope has been the subject of extensive study. Data on the single-crystal elastic tensor of the endmembers and of intermediate compositions are available in the literature [*Sinogeikin and Bass*, 2000, 2002]. The calculated sensitivities of the seismic velocities to the pyrope content are both positive, $\partial \ln v_P/\partial X_{Al} = 0.03 \pm 0.01$, $\partial \ln v_S/\partial X_{Al} = 0.04 \pm 0.01$, where $X_{Al} = Al/(Al+Mg^{VI}+Si^{VI})$, and Mg^{VI} and Si^{VI} refer to atoms in octahedral coordination. This effect is about 5 times smaller than the effect of Al enrichment in orthopyroxenes. The logarithmic derivatives of velocity with respect to density related to Al enrichment in majoritic garnets are positive, $\partial \ln v_P/\partial \ln \rho = 1.2 \pm 0.2$, $\partial \ln v_S/\partial \ln \rho = 1.5 \pm 0.2$ (Table 5).

Recent results on polycrystalline Al-bearing Mg silicate perovskite [*Jackson et al.*, 2004] show that Al- enrichment produces a large R value at ambient conditions, in contrast with the results for orthopyroxenes and pyrope-majorite.

3.2.5. Periclase–wüstite mixture. Periclase (MgO)–wüstite (FeO) solid solution represents the second most abundant mineral in the lower mantle in the reference mineralogical model of the Earth [e.g. *Jackson*, 1988]. A study of the single-crystal elasticity of the complete solid solution series has been performed at ambient conditions by *Jacobsen et al.* [2002] using GHz-ultrasound interferometry. Periclase has been subject of numerous single-crystal studies at both high-pressure and high-temperature [e.g. *Jackson and Niesler*, 1982; *Chen et al.*, 1998; *Sinogeikin and Bass*, 2000]. The strong nonlinearity in the compositional dependence of the shear modulus causes a compositional dependence of both compressional and shear velocity heterogeneity parameters. However, because the role of nonstoichiometry and defect density in the Fe-rich members of the series remains unclear [e.g. *Jacobsen et al.*, 2002], we limit our estimation to the first order effect only. Our computed heterogeneity parameters are $\partial \ln v_P/\partial X_{Fe} = -0.46 \pm 0.05$, and $\partial \ln v_S/\partial X_{Fe}$

= -0.74 ± 0.07. Both compressional and shear velocity heterogeneity parameters in periclase–wüstite are the largest among the whole set of minerals examined in this study. Moreover, they are much larger than $\partial \ln v_P/\partial X_{Fe}$ = -0.16, and $\partial \ln v_S/\partial X_{Fe}$ = -0.22, calculated by first principles for $(Mg,Fe)SiO_3$ perovskite, the other principal component of the lower mantle [*Kiefer et al.*, 2002].

On balance, we find that the heterogeneity parameter for a single substitution such as Fe–Mg can vary dramatically for different mantle mineral families. The logarithmic compositional heterogeneity parameters for v_P and v_S can vary by a factor of ~10, depending on the mineral structure involved (Table 5).

3.3. Temperature Versus Pressure Effects: Experimental Results

Reliable mineralogical models of the Earth interior must integrate high-temperature and high-pressure experimental results from mineral physics in a coherent thermodynamic and petrological model in order to compute single phase and rock aggregate properties along pressure–temperature–composition paths relevant to the Earth interior. The available high-quality high-temperature elasticity studies performed by resonant ultrasound spectroscopy (see *Anderson and Isaak* [1995] for reference) and by Brillouin spectroscopy [e.g. *Sinogeikin et al.*, 2003] combined with high-pressure results on comparable mineral phases, allow us to separately investigate temperature and pressure effects on the compositional sensitivity of acoustic velocity in three solid solution series: forsterite–fayalite, pyrope–grossular, and ringwoodite–γ-Fe_2SiO_4. The average relative uncertainties on the pressure and temperature derivatives of the elastic moduli from selected high-quality single-crystal measurements (Tables 1, 2) are always less than 10% and very often smaller than the uncertainties associated with results of other techniques, such as high-pressure and high-temperature polycrystalline ultrasonics and X-ray diffraction [e.g. *Liebermann*, 2000; *Jiang et al.*, 2004 b].

The temperature and pressure effects of Fe–Mg substitution in olivine and ringwoodite–γ-Fe_2SiO_4 and Ca–Mg substitution in pyrope–grossular are plotted in Figure 4 as relative variation with respect to the heterogeneity parameter, $\Delta v/(v\Delta X_{Fe})$ computed at ambient conditions (Table 5). The experimental results are extrapolated, when needed, using an approach based on Grüneisen theory [e.g. *Duffy and Anderson*, 1989].

In olivine, the pressure and temperature effects have an opposite sign, suggesting a near cancellation of pressure-temperature effects under mantle conditions (Figure 4a, b). In γ-phase (Figure 4c, d) pressure increase causes a negligible decrease of both $\partial \ln v_P/\partial X_{Fe}$ and $\partial \ln v_S/\partial X_{Fe}$, while the effect of temperature is to decrease $\partial \ln v_P/\partial X_{Fe}$ as much as 35% and increase $\partial \ln v_S/\partial X_{Fe}$ up to 40% at T = 1800 K. The comparison between the two minerals suggests that the Fe to Mg substitution is more effective in decreasing the shear stiffness of the denser γ-phase than that of olivine.

In grossular–pyrope solid solutions, temperature increases $\partial \ln v_P/\partial X_{Ca}$ up to 20% at 1800 K and the effect on $\partial \ln v_S/\partial X_{Ca}$ is to decrease its value by 15% at 1800 K with a variation of the heterogeneity ratio $R = \partial \ln v_S/\partial \ln v_P$ from 2.2 at 300 K to 1.9 at 1800 K. The effect of pressure is that of decreasing both the heterogeneity parameters. However, the effect on the compressional velocity is two times larger than that observed on the shear velocity causing an increase of the heterogeneity ratio R to 2.5 at 10 GPa and 300 K (Figure 4 e,f). This behavior is in good agreement with our results for Ca–Mg substitution in ternary garnet with Fe contents consistent with peridotitic compositions (see section 3.1).

The available data suggest that temperature and pressure dependence of the heterogeneity parameters for the same chemical substitution can be radically different even in closely related systems such as olivine and its high-pressure polymorph γ-phase, suggesting caution in generalizing results obtained at ambient pressure and temperature by direct extrapolation to the conditions and the materials of the deep Earth's interior. The combination of high-quality data collected at high temperature and high pressure is the prerequisite to any reliable modeling or even qualitative estimation of the compositional effect on seismic velocity under mantle conditions. However, in general, the effects of P and T at upper mantle conditions on heterogeneity parameters are smaller than the changes in heterogeneity parameters observed across the different structure types.

3.4. The Effect of Water

The effect of water content on the elastic property of minerals of the mantle is far from being completely explored experimentally. The very few single-crystal elasticity studies of hydrated silicates give us a general idea limited to the olivine system, to γ-phase and grossular [e.g. *Wang et al.*, 2003]. Superhydrous phase B and phase D, two of the high-pressure magnesium silicate hydrous phases which are considered the most probable carriers of water in the deep interior of the Earth, have been subject of single-crystal elasticity measurements by *Pacalo and Weidner* [1996] and *Liu et al.* [2004] respectively. Here we report estimates of the average sensitivity of seismic velocity to water content in the cases of γ-phase and grossular, in which water incorporation does not involve structural modifications (Table 6). We also determine average sensitivities to water content by comparison of Mg-rich olivine with humite-group minerals

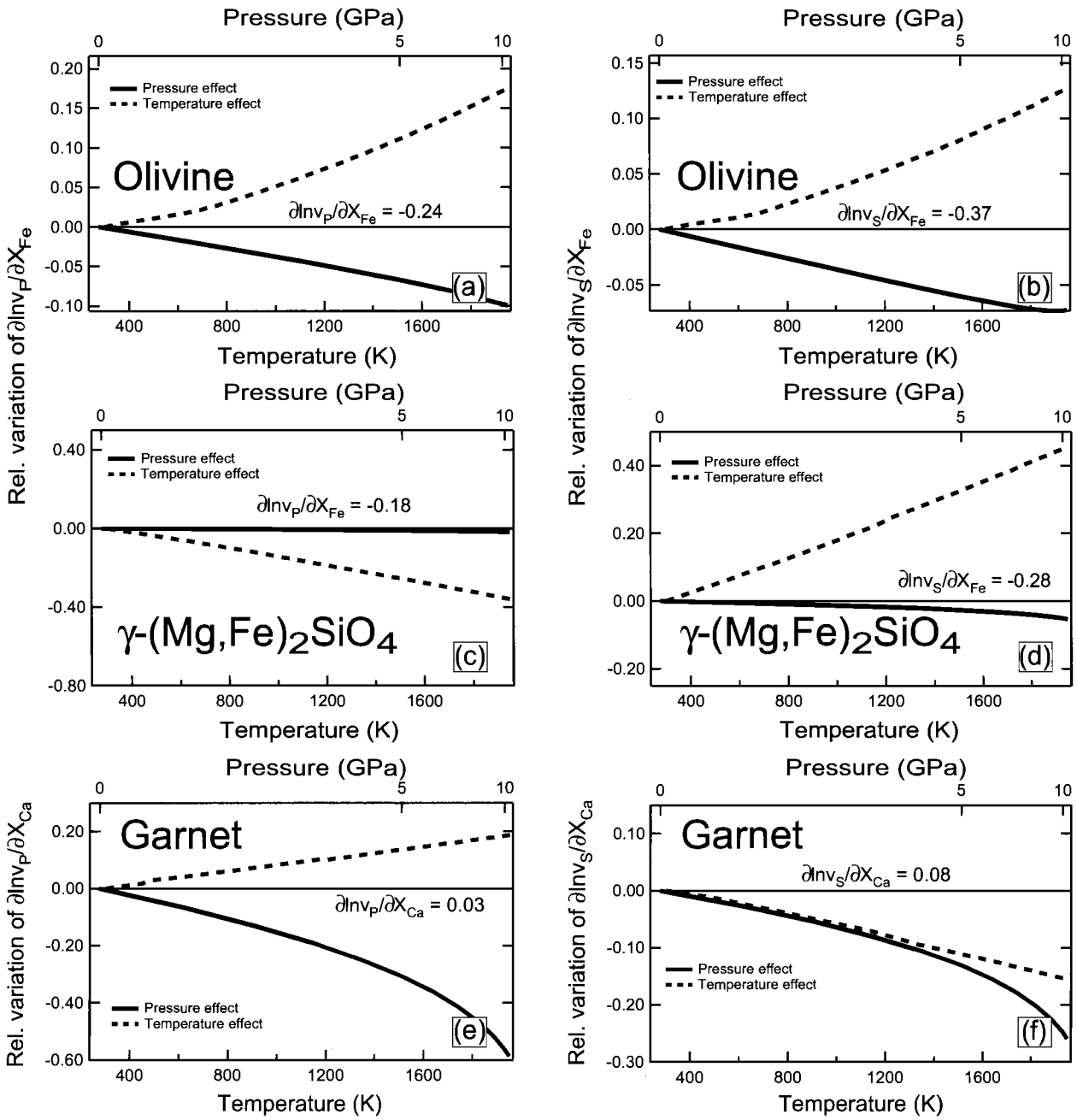

Figure 4. Temperature and pressure dependences of the elastic wave velocity compositional heterogeneity parameters from direct experiments for olivine (a, b), ringwoodite–γ-Fe2SiO4 (c, d), and grossular–pyrope garnets (e, f). Pressure and temperature effects are expressed as relative variations with respect to the heterogeneity parameters at ambient conditions. The pressure scale is not linear so as to match the temperature scale in agreement with the mantle geotherm by *Gasparik and Hutchison* [2000]. Data for olivine are from *Sumino* [1979], *Isaak et al.* [1989], *Isaak* [1992], *Zha et al.* [1996, 1998], *Abramson et al.* [1997], and *Speziale and Duffy* [2004]. Data for ringwoodite–γ-Fe2SiO4 are from *Jackson et al.* [2000] and *Sinogeikin et al.* [2003]. Data for pyrope–grossular are from *Suzuki and Anderson* [1983], *Isaak et al.* [1992], *Sinogeikin and Bass* [2000], and *Jiang et al.* [2004 b].

and of MgO with $Mg(OH)_2$, which instead represent systems where hydration involves structural modifications (Table 6). In this study all the different systems are examined at ambient conditions.

The softening caused by hydration affects in a similar way both compressional and shear velocity. As a consequence, the value of the ratio $R = \partial \ln v_S / \partial \ln v_P$ is equal to 1 for ringwoodite-hydrous ringwoodite, grossular-hydrogrossular, and olivine-humites (Table 6). This effect is different from that of Fe–Mg and Ca–Mg substitutions (Table 5). However, the amplitude of the effect is sensitive to the specific mechanism of water incorporation in the host crystallographic structure (H_4O_4 substitution for SiO_4, or OH substitution for O at the vertices of metal coordination polyhedra). Indeed the heterogeneity parameters in different systems are not immediately comparable in terms of total amount of water in the host mineral (Table 6). The complex interplay of crystallographic structure and density effect, already observed in the case of metal substitutions is also present in the case of OH enrichment, as shown in Table 6.

The results discussed here represent the effect of water content on the heterogeneity parameters in the elastic regime. However, it has been demonstrated that water plays a primary role in enhancing anelastic effects in silicates [e.g. *Karato and Jung*, 1998], which have to be fully taken into account when laboratory elasticity results (obtained using high frequency spectroscopic methods) are compared with seismological observations.

3.5. Applications to Mineralogical Models of the Mantle

3.5.1. Overview. In the prospective of understanding the Earth interior, mineral physics furnishes information about the elastic behavior of candidate mantle minerals at high pressures and temperatures in order to construct mineralogical and petrological models of the Earth that can satisfy both geophysical observation and geochemical constraints. In a first-order approximation, the rocks of the upper mantle contain mineral assemblages consistent with those observed in oceanic peridotites, mantle xenoliths and diamond inclusions [e.g. *Moore and Gurney*, 1985; *Menzies and Dupuy*, 1991; *Griffin et al.*, 1999], which give us a partial sampling mostly of regions shallower than 400 km depth.

Rocks of different origin and compositions contain substantially different minerals assemblages, which are subject to modifications at depth. For this reason, in absence of reliable mineral physics databases, general correlations between elemental enrichments and average sound velocities [e.g. *Lee*, 2003] could result in largely inaccurate model velocities, especially if extrapolated to mantle conditions. As an example of the complexity of the effects of variable rock chemistry, in a pyrolitic average mantle, rich in $(Mg,Fe)_2SiO_4$ polymorphs, the volume fraction of garnet is 15% in the upper mantle and that of garnet-majorite solid solution is 40% in the transition zone [*Fei and Bertka*, 1999], a MORB eclogite, corresponding to subducted oceanic crustal material, contains 25% garnet at the top of the upper mantle but about 90% majorite-garnet solid solution in the transition zone [*Irifune and Ringwood*, 1993]. The relative contribution of garnets to the overall thermoelastic properties of the two rock types, will be dramatically different in varying temperature and pressure regimes. To model the behavior of the rock at mantle conditions the chemical composition has to be accompanied by a precise mineralogical and petrological model.

Single-crystal elastic properties need to be converted into effective or average elastic properties of mineral aggregates in order to compare mineral physics information with information from seismology. Simple bounding schemes for the elastic moduli of isotropic aggregates [*Hill*, 1963; *Hashin and Shtrikman*, 1961; *Watt et al.*, 1976] are often used in geophysical mineralogical models [*Duffy and Anderson*, 1989; *Lee*, 2003, *Cammarano et al.*, 2003]. In the same spirit, we use a very simple approach, described in section 2.4, to determine the average heterogeneity parameters for Fe–Mg substitution in pyrolite, piclogite, and harzburgite and in MORB eclogite (Table 7) along an adiabatic profile with starting temperature of 1673 K up to the bottom of the upper mantle, using information about the compositional sensitivity of seismic velocity in mantle minerals. As a test of our averaging scheme, we applied it to mixtures of garnet and olivine. The consistency of our results with a more rigorous approach based on Hashin–Shtrikman bounds (cf. Section 2.4) demonstrates the reliability of our computed heterogeneity parameters (Plate 1).

3.5.2. Average heterogeneity parameters. The heterogeneity parameters for Fe–Mg substitution calculated for MORB eclogite, which is strongly enriched in garnet-majorite component at high pressure, are $\partial \ln v_P / \partial X_{Fe} = -0.09 \pm 0.02$ and $\partial \ln v_S / \partial X_{Fe} = -0.14 \pm 0.02$ and they gradually decrease with depth to -0.08 ± 0.02 and -0.10 ± 0.02 at the conditions of the transition zone (Plate 2). Pyrolite, piclogite and harzburgite, all characterized by more than 40% olivine or its high-pressure polymorphs, show estimated heterogeneity parameters up to 3 times larger than MORB at ambient pressure (Plate 2). Both $\partial \ln v_P / \partial X_{Fe}$ and $\partial \ln v_S / \partial X_{Fe}$ for these rock types slowly decrease (in absolute value) with pressure within the stability field of olivine, and then more rapidly at the olivine–β-$(Mg,Fe)_2SiO_4$ transition and then increase in magnitude at the β- to γ-transition [*Irifune and Ringwood*, 1987a, b, 1993; *Ita and Stixrude*, 1992]. The ratio $R = \partial \ln v_S / \partial \ln v_P$ of pyrolite,

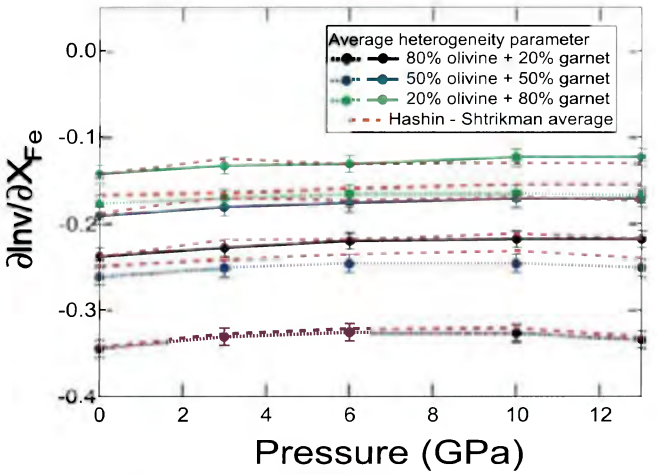

Plate 1. Heterogeneity parameters of binary mixtures of olivine (90 mol% forsterite) and garnet (72 mol% pyrope, 14 mol% almandine, 14 mol% grossular) in different volume ratios. The parameters calculated with our average scheme (see text) are compared with the results of a more formal approach based on Hashin–Shtrikman bounding of the elastic moduli of the mixtures. The results agree within uncertainties. Solid lines: $\partial \ln v_P / \partial X_{Fe}$. Dashed lines: $\partial \ln v_S / \partial X_{Fe}$.

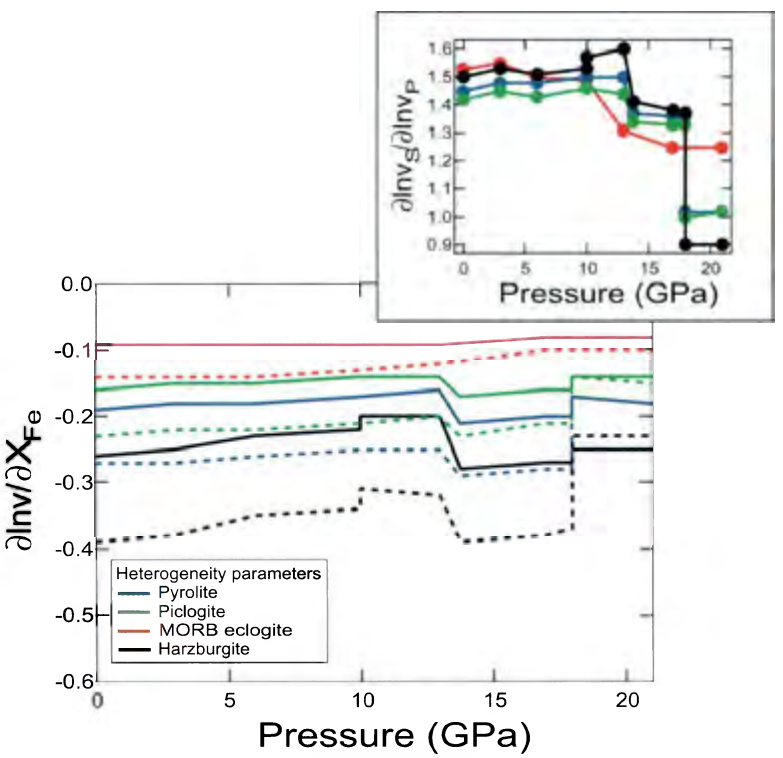

Plate 2. Sensitivity of compressional and shear wave velocities to Fe-–Mg substitution calculated for pyrolite, piclogite, harzburgite, and MORB eclogite, along an isentropic pressure/temperature path with a foot temperature of 1673 K. The modal compositions and stability field boundaries for the different mineral phases in the four rock types were derived from *Irifune and Ringwood* [1987b, 1993], *Ita and Stixrude* [1992], and *Vacher et al.* [1998]. Solid lines: $\partial \ln v_P / \partial X_{Fe}$. Dashed lines: $\partial \ln v_S / \partial X_{Fe}$. Inset: variation of the heterogeneity parameters ratio $R = \partial \ln v_P / \partial \ln v_S$ for the four rock types along the same isentropic pressure/temperature path.

Table 8. Relative Velocity Changes Upon Transitions Between Different Mantle Rock Types.

Rock type	$\Delta v_P/v_P$	$\Delta v_S/v_S$	$\Delta v_B/v_B$	$[\Delta v_S/v_S]/[\Delta v_P/v_P]$
Pyrolite–piclogite	0.005 (2)	0.005 (1)	0.005 (2)	1.0 (3)
Pyrolite–harzburgite	-0.006 (2)	0.001 (3)	-0.012 (3)	-0.2 (3)
Pyrolite–MORB	-0.027 (2)	-0.038 (1)	-0.019 (3)	1.4 (1)
Piclogite–harzburgite	-0.011 (2)	-0.004 (1)	-0.016 (2)	0.4 (1)
Piclogite–MORB	-0.032 (2)	-0.043 (2)	-0.023 (3)	1.4 (1)
MORB–harzburgite	0.022 (2)	0.041 (1)	0.007 (2)	1.9 (2)

piclogite, and harzburgite is dominated by the properties of olivine and its polymorphs. It slowly increases with depth in the upper mantle, ranging between 1.45 ± 0.05 and 1.53 ± 0.05, and then it rapidly decreases in the transition zone to about 1.0 ± 0.1 at the β- to γ-$(Mg,Fe)_2SiO_4$ transition. MORB eclogite, which is enriched in garnet, shows a smaller decrease of the ratio $\partial \ln v_S/\partial \ln v_P$ from 1.5 ± 0.1 in the upper mantle to 1.3 ± 0.1 at the bottom of the transition zone. One reasonable interpretation of these results is that the seismic signature of bulk compositional variation in the olivine-rich rocks of the mantle fades with pressure in the transition zone, while it will remain visible in MORB eclogite.

3.5.3. Effect of elemental partitioning. We have carried out simple calculations of the effect of changes in Fe–Mg partitioning between the different minerals on the elastic velocities of these four rock-types at ambient conditions. The computations have been performed using Hashin–Shtrikman bounds to the rock elastic moduli to determine average rock velocities. The relative velocity variations $\Delta v_i/v_i$, where Δv_i is the velocity difference caused by enrichment of Mg up to 4 mol% in pyroxene at constant rock bulk composition in MORB eclogite, are $\Delta v_P/v_P = 0.002$ and $\Delta v_S/v_S = 0.003$. Similar enrichment in Mg in olivine results in $\Delta v_P/v_P = -0.002$ and $\Delta v_S/v_S = -0.002$ in harzburgite and $\Delta v_P/v_P = 0.002$ and $\Delta v_S/v_S = 0.003$ in pyrolite. We do not resolve a significant variation in piclogite, where the modal abundances of the different minerals are relatively close to one another (Table 7) and the compositional effects cancel out completely. The values of the calculated ratios $(\Delta v_S/v_S)/(\Delta v_P/v_P)$ for the different rock types are in the range 1.0–1.5, comparable to the heterogeneity ratio $R = \partial \ln v_S/\partial \ln v_P$ due to variations of the bulk Fe/Mg ratio in the same rocks. Based on these (indeed limited) results we cannot rule out that variations of the heterogeneity parameters with depth could represent an indicator of the sensitivity of seismic velocity to variations in the partition of Fe between the different mineral phases. Developing this interpretation we could use the heterogeneity parameters for bulk rock compositional changes as qualitative estimates of the heterogeneity determined by transitions between the different rock types in the mantle, which also involve large changes in bulk rock chemical composition and different Fe/Mg ratios in the constituent minerals.

3.5.4. Effect of lateral variations of lithology. We have calculated the effect of transition from one to the other of the four examined rock compositions, as the relative velocity difference $\Delta v_i/v_i$, where v_i is elastic wave velocity at ambient conditions (Table 8). In the transition from pyrolite to MORB eclogite the relative variation $\Delta v_P/v_P$ is -0.027 ± 0.002 and $\Delta v_S/v_S$ is -0.038 ± 0.001 with $(\Delta v_S/v_S)/(\Delta v_P/v_P) = 1.4 \pm 0.1$. The relative changes in compressional and shear velocities between piclogite and MORB eclogite are $\Delta v_P/v_P = -0.032 \pm 0.002$ and $\Delta v_S/v_S = -0.043 \pm 0.002$, both larger than in the case of pyrolite, but the ratio $(\Delta v_S/v_S)/(\Delta v_P/v_P)$ is 1.4 ± 0.1, as for pyrolite. These results are in order of magnitude agreement with the range of calculated variations between different mantle rocks by *Goes et al.* [2000], which are based on a different mineral physics data selection.

The magnitude of the calculated heterogeneity ratios $(\Delta v_S/v_S)/(\Delta v_P/v_P)$ due to the change in Fe–Mg content at the transition between different types of upper mantle rocks are consistent with global seismic models [e.g. *Masters et al.*, 2000]. However, our results do not take explicitly into account the effect of Al substitution for Mg and Fe, whose effect cannot be modeled based on the limited available single-crystal elasticity data.

Using the heterogeneity parameters calculated for bulk rock variations of Fe/Mg ratio as an approximation of $(\Delta v_S/v_S)/(\Delta v_P/v_P)$ upon transitions between the different rocks (see discussion above), we estimate that this ratio decreases at depths of the transition zone, in agreement with the decreasing values of $\partial \ln v_S/\partial \ln v_P$ from 1.5 to 1.2 determined in the transition zone by a careful analysis of matching P and S data for global tomographic images [*Saltzer et al.*, 2001].

We finally compare our results with those of *Lee* [2003], by computing density, elastic wave velocity, and their loga-

rithmic variation with respect to bulk Mg#, defined as the molar ratio Mg/(Mg + Fe), in "synthetic" garnet peridotite compositions that we calculated by small perturbations of the composition of natural peridotites, and their mineral phases selected from the databases used in that study. In order to obtain a stable fit of the compositional sensitivities of the different parameters, we computed 15,000 rock compositions, selected such that both the single mineral phases and the whole rock are within the ranges of Mg# of the dataset used by *Lee* [2003]. Our computed logarithmic dependence of shear velocity on Mg#, $\partial \ln v_S/\partial Mg\# = 3.45 \times 10^{-3}$, is 15% larger than the results of *Lee* [2003] (Table 9). Our results indicate that the compressional velocity has a logarithmic dependence $\partial \ln v_P/\partial Mg\# = 2.14 \times 10^{-3}$, similar to that of v_S, but with larger uncertainty. The larger scatter of longitudinal velocity was also observed by *Lee* [2003]. However, the average compositional dependence of v_P on Mg# is in disagreement with the results of *Lee* [2003], as it is demonstrated by the different compositional sensitivity of the ratio v_P/v_S, which is 45% smaller than that proposed by *Lee* [2003] (Table 9).

Table 9. Compositional Sensitivity of the Acoustic Wave Velocity in Garnet Peridotites.

Derivative	This study	*Lee* [2003]
$100 \times \partial \ln v_P/\partial Mg\#$	0.214 (5)	---
$100 \times \partial \ln v_S/\partial Mg\#$	0.345 (5)	0.30 (2)
$100 \times \partial (v_P/v_S)/\partial Mg\#$	-0.224 (5)	-0.41 (4)

---, parameter not determined.

4. CONCLUSIONS

Global seismological and geodynamical models require an assessment not only of thermal effects but also of compositional effects on the elastic properties of the constituents of the Earth. Based on the available single-crystal elasticity data we have shown that it is possible to develop a dataset of compositional sensitivities of the main candidate minerals of the mantle. Our principal results are:

(1) Logarithmic velocity variations with respect to iron content are very sensitive to crystal structure, pressure, and temperature. At ambient conditions, $\partial \ln v_P/\partial X_{Fe}$ for garnets, olivines (including high-pressure polymorphs), pyroxenes, and periclase-wüstite ranges from -0.05 to -0.46, whereas $\partial \ln v_S/\partial X_{Fe}$ ranges from -0.08 to -0.74. The effects of pressure and temperature can change these values markedly under upper mantle conditions, but P-T effects vary greatly from structure to structure, and no general rules about the effects of pressure and temperature can be formulated.

(2) α- and γ- poymorphs of $(Mg,Fe)_2SiO_4$ exhibit broadly comparable values of $\partial \ln v/\partial X_{Fe}$ at ambient conditions, but the temperature dependences of these quantities are large and of opposite sign between the two polymorphs.

(3) Of the mineral families investigated for Fe–Mg substitution, the (Mg,Fe)O series is the most sensitive to chemical substitution showing $\partial \ln v_P/\partial X_{Fe} = -0.46 \pm 0.05$ and $\partial \ln v_S/\partial X_{Fe} = -0.74 \pm 0.07$, whereas garnets are the least sensitive, with $\partial \ln v_P/\partial X_{Fe} = -0.09 \pm 0.01$ and $\partial \ln v_S/\partial X_{Fe} = -0.08 \pm 0.01$.

(4) Al and Ca enrichments increase seismic velocities in orthopyroxenes, ternary garnets, and majorite garnets. The magnitude of the effect of Al incorporation in orthopyrene produces much larger changes in velocity ($\partial \ln v_P/\partial X_{Al} = 0.24 \pm 0.04$ and $\partial \ln v_S/\partial X_{Al} = 0.13 \pm 0.04$) than Al substitution in majorites ($\partial \ln v_P/\partial X_{Al}$ and $\partial \ln v_S/\partial X_{Al} \leq 0.04$) or Ca in garnets ($\partial \ln v_P/\partial X_{Fe}$ and $\partial \ln v_S/\partial X_{Fe} \leq 0.08$).

(5) Values of $\partial \ln v_S/\partial \ln v_P$ resulting from Fe–Mg substitution in different mineral families range from 0.9 to 1.7. A very large value of the heterogeneity ratio ($\partial \ln v_S/\partial \ln v_P = 2.7 \pm 0.6$) is found only for Ca–Mg substitution in ternary garnets at ambient conditions

(6) The effect of hydration in grossular and ringwoodite and in the systems olivine–humites, and periclase–brucite is to decrease both compressional and shear velocity, with $\partial \ln v_S/\partial \ln v_P$ ranging between 1.0 and 1.3.

(7) In a simplified model of rock behavior, the very different response of garnets and olivines to Fe substitution gives rise to variations in the sensitivity of different rocks to iron concentration in accordance to their garnet content. For instance, velocities in mid-ocean ridge eclogites are about 2–3 times less sensitive to iron enrichment than those in harzburgites. Due to their enrichment in olivine component, values of $\partial \ln v_S/\partial \ln v_P$ of pyrolite, piclogite and harzburgite as a result of chemical substitution show a decrease from 1.5 ± 0.1 in the upper mantle to 1.0 ± 0.1 in the transition zone. MORB eclogite, which is extremely enriched in garnet component, shows a smaller decrease of $\partial \ln v_S/\partial \ln v_P$ from 1.5 ± 0.1 to 1.3 ± 0.1.

(8) The sensitivity of seismic velocities of pyrolite, harzburgite and MORB eclogite to change in Fe/Mg partitioning between the constituent minerals is one order of magnitude smaller than the effect of variation of the bulk rock composition. No clear effect is detected in piclogite. The heterogeneity parameters ratios $R = \partial \ln v_S/\partial \ln v_P$ are broadly comparable with those relative to bulk rock enrichment/depletion in Fe.

(9) Using the sensitivity to bulk compositional change in Fe content, and its pressure dependence, as a proxy for the

heterogeneity parameters upon transitions between the different mantle rock-types we estimate that the intensity of the seismic effect of the transition from average mantle to subducted slab rocks progressively fades at transition zone depths.

In order to have internal consistency in the selection of the whole set of parameters reported in this study, we have selected only single-crystal elasticity measurements, excluding many polycrystalline elasticity and X-ray diffraction results. The drawback of this choice is that it reduced our ability to give a complete description of the pressure/temperature dependence of the elastic properties of the examined minerals. On the other hand, the unavoidable inconsistency between the results from different techniques, the limitations of parameters deduced by approximate elasticity systematics, and the poor resolution of moduli constrained as fit parameters of standard equations of state (as in the case of bulk modulus and its pressure and temperature derivatives from X-ray diffraction experiments) suggest caution in interpreting the results based on the use of partially outdated or extensive but inconsistent elasticity databases. New perspectives in the interpretation of the properties of the Earth's mantle are represented by self-consistent thermodynamic models [e.g. Stixrude and Lithgow-Bertelloni, 2005] applied to a homogeneous (possibly single-crystal) elasticity database, and compatible with the mineralogical and petrological experimental constraints.

Acknowledgments. The authors thank two anonymous reviewers for their thoughtful comments and suggestions that helped to improve the original manuscript. S. S. thanks R. Jeanloz for the helpful discussions and the Miller Institute for Basic Research in Science that is supporting his work at the University of California at Berkeley.

REFERENCES

Abramson, E. H., J. M. Brown, L. J. Slutsky, and J. Zaug (1997), The elastic constants of San Carlos olivine to 17 GPa, *J. Geophys. Res., 102*, 12253–12263.

Akaogi, M., and S. Akimoto (1979), High-pressure phase equilibria in a garnet lherzolite, with special reference to Mg^{2+}-Fe^{2+} partitioning among constituent minerals, *Phys. Earth Planet. Inter., 19*, 31–51.

Anderson, D. L., and J. D. Bass (1986), Transition region of the Earth's upper mantle, *Nature, 320*, 321–328.

Anderson, O. L., and D. G. Isaak (1995), Elastic constants of mantle minerals at high temperature, in *Mineral physics and crystallography. A handbook of physical constants, AGU Reference shelf* 2, edited by T. J . Ahrens, pp.64–97, AGU, Washington D.C.

Angel, R. J. (2000), Equations of state, in *High-Temperature and High-Pressure Crystal Chemistry, Reviews in Mineralogy and Geochemistry*, vol. 41, edited by R. M. Hazen and R. T. Downs, pp. 35–59, Mineralogical Society of America, Washington D.C.

Antolik, M., Y. J. Gu, G. Ekström, and A. M. Dziewonski (2003), J362D28: a new joint model of compressional and shear velocity in the Earth's mantle, *Geophys. J. Inter., 153*, 443–466.

Armbruster, T., C. A. Geiger, and G. A. Lager (1992), Single-crystal X-ray structure study of synthetic pyrope almandine garnets at 100 and 293 K, *Am. Mineral., 77*, 512–521.

Babuška, V., J. Fiala, M. Kumazawa, I. Ohno, and Y. Sumino (1978), Elastic properties of garnet solid-solution series, *Phys. Earth Planet. Inter., 16*, 157–176.

Bass J. D. (1986), Elasticity of uvarovite and andradite garnets, *J. Geophys. Res.*, 91, 7505–7516.

Bass, J. D. (1989), Elasticity of grossular and spessartine garnets by Brillouin spectroscopy, *J. Geophys. Res., 94*, 7621–7628.

Bass, J. D., and D. L. Anderson (1984), Composition of the upper mantle: geophysical tests of two petrological models, *Geophys. Res. Lett., 3*, 237–240.

Bass, J. D., and M. Kanzaki (1990), Elasticity of majorite-pyrope solid solution, *Geophys. Res. Lett., 97*, 4809–4822.

Bass, J. D., and D. J. Weidner (1984), Elasticity of single-crystal orthoferrosilite, *J. Geophys. Res., 89*, 4359–4371.

Beckman Fritzel, T. L., and J. D. Bass (1997), Sound velocity of clinohumite, and implications for water in Earth's upper mantle, *Geophys. Res. Lett., 24*, 1023–1026.

Cammarano, F., S. Goes, P. Vacher, and D. Giardini (2003), Inferring upper-mantle temperatures from seismic velocities, *Phys. Earth Planet. Inter., 138*, 197–222.

Chai, M, J. M. Brown, and L. J. Slutsky (1997), The elastic constants of an aluminum orthopyroxene to 12.5 GPa, *J. Geophys. Res., 102*, 14,779–14,785.

Chen, G., R. C. Liebermann, and D. J. Weidner (1998), Elasticity of single-crystal MgO to 8 gigapascal and 1600 K, *Science, 280*, 1913–1916.

Collins, M.D., and J. M. Brown (1998), Elasticity of an upper mantle clinopyroxene, *Phys. Chem. Minerals, 26*, 7–13.

Davies, G. F, and A. M. Dziewonski (1975), Homogeneity and constitution of the Earth's lower mantle and outer core, *Phys. Earth Planet. Inter., 10*, 336–343.

Duffy T. S., and D. L. Anderson (1989), Seismic velocities in mantle minerals and the mineralogy of the upper mantle, *J. Geophys. Res., 94*, 1895–1912.

Duffy, T. S., and M. T. Vaughan (1988), Elasticity of enstatite and its relationship to crystal structure, *J. Geophys. Res., 93*, 383–391.

Fei, Y. (1995), Thermal expansion, in *Mineral physics and crystallography. A handbook of physical constants, AGU Reference shelf* 2, edited by T. J. Ahrens, pp.29–44, AGU, Washington D.C. 64–97.

Fei, Y., and C. M. Bertka (1999), Phase transitions in the Earth's mantle and mantle mineralogy, in *Mantle Petrology: Field Observations and High Pressure Experimentation, Special Publication* No. 6, edited by Y. Fei, C. M. Bertka, and B. O. Mysen, pp.189–207, The Geochemical Society, Houston.

Forte, A. M., and J. X. Mitrovica (2001), Deep-mantle high-viscosity flow and thermochemical structure inferred from seismic and geodynamic data, *Nature*, 410, 1049–1056.

Forte, A. M., and R. Woodward (1997), Seismic-geodynamic constraints on three-dimensional structure, vertical flow, and heat transfer in the mantle, *J. Geophys. Res., 102*, 17,981–17994.

Forte, A. M., and H. K. C. Perry (2000), Geodynamic evidence for a chemical depleted continent tectosphere, *Science, 290*, 1940–1944.

Frisillo, A. L., and G. R. Barsch (1972), Measurement of single-crystal elastic constants of bronzite as a function of pressure and temperature, *J. Geophys. Res., 77*, 6360–6384.

Gasparik, T., and M. T. Hutchison (2001), Experimetnal evidence for the origin of two kinds of inclusions in diamonds from the deep mantle, *Earth Planet. Sci. Letters, 181*, 103–114.

Geiger, C. A. (1999), Thermodynamics of $(Fe^{2+},Mn^{2+},Mg^{2+},Ca)_3Si_3O_{12}$ garnet: An analysis and a review, *Mineral. Petrol., 66*, 271–299.

Goes, S., R. Govers, and P. Vacher (2000), Shallow mantletemperatures under Europefrom P and S wavetomography, *J. Geophys. Res., 105*, 11153–11169.

Graham, E. K., J. A. Schwab, S. M. Sopkin, and H. Takei (1988), The pressure and temperature dependence of the elastic properties of single-crystalfayalite Fe2SiO4, *Phys. Chem. Minerals*, 16, 186–198.

Grand, S. P, R.D. van der Hilst, and S. Widiyantoro (1997), Global seismic tomography: a snapshot of convection in the Earth, *GSA Today, 7*, 1–7.

Griffin, W. L., S. Y. O'Reilly, and C. G. Ryan (1999), The composition of sub-continental lithospheric mantle, in *Mantle Petrology: Field Observations and High Pressure Experimentation, Special Publlication* No. 6, edited by Y. Fei, C. M. Bertka, and B. O. Mysen, pp. 13–45, The Geochemical Society, Houston.

Gung, Y., M. Panning, and B. Romanowicz (2003), Global anisotropy and the thickness of continents, *Nature, 422*, 707–711.

Hashin, Z., and S. Shtrikman (1961), Note on a variational approach to the theory of composite elastic materials, *J. Franklin Inst., 271*, 336–341.

Hashin, Z., and S. Shtrikman (1963), A variational approach to the elastic behavior of multiphase materials, *J. Mech. Phys. Solids, 11*, 127–140.

Hill, R. (1963), Elastic properties of reinforced solids: Some theoretical principles, *J. Mech. Phys. Solids, 11*, 357–372.

Inoue, T., D. J. Weidner, P. A. Northrup, and J. B. Parise (1998), Elastic properties of hydrous ringwoodite (γ-phase) in Mg_2SiO_4, *Earth Planet. Sci. Lett., 160*, 107–113.

Irifune, T., and M. Isshiki (1998), Iron partitioning in a pyrolite mantle and the nature of the 410-km seismic discontinuity, *Nature, 392*, 702–705.

Irifune, T., and A. E. Ringwood (1987a), Phase transformations in primitive MORB and pyrolite compositions to 25 GPa and some geophysical implications, in *High Pressure Research in Geophysics*, edited by M. H. Manghnani and Y. Syono, pp. 231–242, Terrapub, AGU, Tokyo, Washington D.C.

Irifune, T., and A. E. Ringwood (1987b), Phase transformations in a harzburgite composition to 26 GPa: Implications for dynamical behavior of the subducting slab, *Earth Planet. Sci. Lett., 86*, 365–376.

Irifune, T., and A. E. Ringwood (1993), Phase transformation in subducted oceanic crust and buoyancy relationships at depths of 600–800 km in the mantle, *Earth Planet. Sci. Lett., 117*, 101–110.

Irifune, T., T. Sekine, A. E. Ringwood, and W. O. Hibberson (1986), The eclogite-garnetite transformation at high pressure and some geophysical implications, *Earth Planet. Sci. Lett., 77*, 245–256.

Isaak, D. G., O. L. Anderson, T. Goto, and I. Suzuki (1989), Elasticity of single-crystal forsterite measured to 1700 K, *J. Geophys. Res., 94*, 5895–5906.

Isaak, D. G., O. L. Anderson, and H. Oda (1992), High-temperature thermal expansion and elasticity of calcium-rich garnets, *Phys. Chem. Miner., 19*, 106–120.

Isaak, D. G., and E. K. Graham (1976), The elastic properties of an almandine-spessartine garnet and elasticity in the garnet solid solution series, *J. Geophys. Res., 81*, 2483–2489.

Isaak, D. G., E. K. Graham, J.D. Bass, and H. Wang (1993), The elastic properties of single-crystal fayalite as determined by dynamical measurements techniques, *Pure Appl. Geophys. 141*, 393–414.

Isaak, D. G., and I. Ohno (2003), Elastic constants of chrome-diopside: application of resonantultrasound spectroscopic to monoclinic single-crystals, *Phys. Chem. Minerals, 30, 430–439.*

Ita, J., and L. Stixrude (1992), Petrology, elasticity and composition of the mantle transition zone, *J. Geophys. Res., 97*, 6849–6866.

Ita, J., and L. Stixrude (1993), Density and elasticity of model upper mantle compositions and their implications for whole mantle structure, in *Evolution of the Earth and Planets, Geophysical Monograph* 74, edited by E. Takahashi, R. Jeanloz and D. Rubie, pp. 111–130, International Union of Geodesy and Geophysics and American Geophysical Union, Washington, D. C.

Jackson, I., and H. Niesler (1982), The elasticity of periclase to 3 GPa and some geophysical implications, in *High Pressure Research in Geophysics*, edited by S. I. Akimoto and M. H. Manghnani, pp.93–113, Cent. for Acad. Publ., Tokyo.

Jackson, J. M., S. V. Sinogeikin, and J.D. Bass (1999), Elasticity of $MgSiO_3$ orthoenstatite, *Am. Mineral., 84*, 677–680.

Jackson, J. M., S. V., S. V. Sinogeikin, and J.D. Bass (2000), Sound velocities and elastic properties of γ-Mg2SiO4 to 873 K by Brillouin spectroscopy, *Am. Mineral., 85*, 296–303.

Jackson, J. M., J. Zhang, and J.D. Bass (2004), Sound velocities and elasticity of aluminous MgSiO3 perovskite: Implications for aluminum heterogeneity in Earth's lower mantle, Geophys. Res. Lett., 31, L10614, doi:10.1029/2004GL019918.

Jacobsen, S.D., H. J. Reichmann, H. A. Spetzler, S. J. Mackwell, J. R. Smyth, R. J. Angel, and C. A. McCammon (2002), Structure and elasticity of single-crystal (Mg,Fe)O and a new method of generating shear waves for gigahertz ultrasonic interferometry, *J. Geophys. Res., 107*, Art. 2037.

Jiang, F., S. Speziale, R. S. Shieh, and T. S. Duffy (2004a), Single crystal elasticity of andradite garnet to 11 GPa, *J. Phys. Condens. Matter, 16*, S1041–S1052.

Jiang, F., S. Speziale, and T. S. Duffy (2004b), Single-crystal elasticity of grossular- and almandine-rich garnets to 12 GPa by Brillouin spectroscopy, *J. Geophys. Res., 109*, B10210, doi:10.1029/2004JB003081.

Jordan, T. H. (1978), Composition and development of the continental tectosphere, *Nature, 274*, 544–548.

Jordan, T. H. (1979), Mineralogies, densities and seismic velocities of garnet lherzolites and their geophysical implications, in *The Mantle Sample: Inclusions in Kimberlites and Other Volcanics, Proceedings of the Second Interantional Kimberlite Conference*, vol. 2, edited by F. R. Boyd, and H. O. Meyer, , pp. 1–14, AGU, Washington D.C.

Kandelin, J., and D. J. Weidner (1988), Elastic properties of hedenbergite, *J. Geophys. Res., 93*, 1063–1072.

Karato, S-I. (1993), Importance of anelasticity in the interpretation of seismic tomography, *Geophys. Res. Lett., 20*, 1623–1626.

Karato, S-I., and H. Jung (1988), Water, partial melting and the origin of the seismic low velocity and high attenuation zone in the upper mantle, *Earth Planet. Sci. Lett., 157*, 193–207.

Karato, S-I., and B. B. Karki (2001), Origin of lateral variation of seismic wave velocities and density in the deep mantle, *J. Geophys. Res., 106*, 21,771–21,783.

Kennett, B. L. N., S. Widiyantoro, and R.D. van der Hilst (1988), Joint seismic tomography for bulk sound and shear wave speed in the Earth's mantle, *J. Geophys. Res., 103*, 12,469–12,493.

Kiefer, B., L. Stixrude, and R. M. Wentzcovitch (2002), Elasticity of $(Mg,Fe)SiO_3$-perovskite at high pressure, *Geophys. Res. Lett., 29*, 10.1029/20002GL014683.

Kumazawa, M. (1969), The elastic constants of single-crystal orthopyroxene, *J. Geophys. Res., 74*, 5973–5980.

Lee, C-T. A. (2003), Compositional variation of density and seismic velocities in natural peridotites at STP conditions: Implications for seismic imaging of compositional heterogeneities in the upper mantle, *J. Geophys. Res., 108*, 2441, doi:10.1029/2003JB002413.

Liebermann, R. C. (2000), Elasticity of mantle minerals (experimental studies), in *Earth's Deep Interior: Mineral Physics and Tomography From the Atomic to the Global Scale, Geophys. Monogr. Ser.*, vol. 117, edited by S-I. Karato , A. Forte, R. Liebermann, G. Masters, and L. Stixrude, pp. 181–199, AGU, Washington D.C.

Liu, L. G., K. Okamoto, Y. J. Yang, C. C. Chen, and C. C. Lin (2004), Elasticity of single-crystal phase D (adense hydrous magnesiumsilicate)by Brillouin spectroscopy, Solid State Comm., 132, 517–520.

Masters, G., G. Laske, H. Bolton, and A. M. Dziewonski (2000), The relative behavior of shear velocity, bulk sound speed, and compressional velocity in the mantle: Implications for chemical and thermal structure, in *Earth's Deep Interior: Mineral Physics and Tomography From the Atomic to the Global Scale, Geophys. Monogr. Ser.*, vol. 117, edited by S-I. Karato , A. Forte, R. Liebermann, G. Masters, and L. Stixrude, pp. 63–87, AGU, Washington D.C.

McDonough, W. F., and R. L. Rudnick (1998), Mineralogy and composition of the upper mantle, in *Ultrahigh-Pressure Mineralogy: Physics and Chemistry of the Earth's Deep Interior, Reviews in Mineralogy, vol. 37*, edited by R. J. Hemley, pp. 139–164, Min. Soc. Am., Washington, D.C.

Menzies, M. A., and C. Dupuy (1991), Orogenic massifs: protolith, process and provenance, *J. Petrol. Spec. Lherzolites Issue,* edited by M. A. Menzies, C. Dupuy, and A. Nicolas, pp. 1–16, Oxford University Press, New York.

Moore, R. O., and J. J. Gurney (1985), Pyroxene solid solution in garnets included in diamond, *Nature, 335*, 784–789.

Novack, G. A., and G. V. Gibbs (1971), The crystal chemistry of the silicate garnets, *Am. Mineral., 56*, 791–825.

Pacalo, R. E. G., and D. J. Weidner (1996), Elasticity of superhydrous B, *Phys. Chem. Minerals, 23*, 520–525.

O'Neill, B., J.D. Bass, J. R. Smyth, and M. T. Vaughan (1989), Elasticity of a grossular-pyrope-almandine garnet, *J. Geophys. Res., 94*, 17,819–17,824.

O'Neill, B., J.D. Bass, G. R. Rossman, C. A. Geiger, and K. Langer (1991), Elastic properties of pyrope, *Phys. Chem. Miner., 17*, 617–621.

O'Neill, B., J.D. Bass, and G. M. Rossman (1993), Elastic properties of hydrogrossular garnet and and implications for water in the upper mantle, *J. Geophys. Res., 98*, 20,031–10,037.

Rigden, S. M., and I. Jackson (1991), Elasticity of germanate and silicate spinels at high pressure, *J. Geophys. Res., 96*, 9999–10,006.

Rigden S. M., G.D. Gwanmesia, I. Jackson, R. C. Liebermann (1992), Progress in high-pressure ultrasonic interferometry, the pressure dependence of elasticity of Mg_2SiO_4 polymorphs and constraints on the composition of the transition zone of the Earth mantle, in *High-Pressure Research: Application to Earth and Planetary Science, Geophys. Monogr. Ser.*, vol. 67, edited by Y. Syono and M. H. Manghnani, pp.167–182, AGU, Washington D.C.

Ringwood, A. E. (1975), *Composition and Petrology of the Earth Mantle*, McGraw-Hill, New York.

Saltzer, R. L., R.D. van Der Hilst, and H. Kárason (2001), Comparing P and S wave heterogeneity in the mantle, *Geophys. Res. Lett., 28*, 1335–1338.

Sawamoto, H., D. J. Weidner, S. Sasaki, and M. Kumazawa (1984), Single-crystal elastic properties of the modified spinel(β) phase of magnesium orthosilicate, *Science, 224*, 749–751.

Sinogeikin, S. V., J.D. Bass, A. Kavner, R. Jeanloz (1997), Elasticity of natural majorite and ringwoodite from the Catherwood meteorite, *Geophys. Res. Lett., 24*, 3265–3268.

Sinogeikin, S. V., and J.D. Bass (1999), Single-crystal elastic properties of chondrodite,: implications for water in the upper mantle, *Phys. Chem. Minerals, 26*, 297–303.

Sinogeikin, S. V., J.D. Bass (2000), Single-crystal elasticity of pyrope and MgO to 20 GPa by Brillouin scattering in the diamond anvil cell, *Phys. Earth Planet. Inter. 120*, 43–62.

Sinogeikin, S. V., and J.D. Bass (2002), Elasticity of majorite and a majotite-pyrope solid solution to high pressure: implications for the transition zone, Geophys. Res. Lett., 29, 10.1029/2001GL013937.

Sinogeikin, S. V., J.D. Bass, and T. Katsura (2003), Single-crystal elasticity of ringwoodite to high pressures and high temperatures: implications for 520 km seismic discontinuity, *Phys. Earth. Planet. Inter., 136*, 41–66.

Sinogeikin, S. V., D. L. Lakshtanov, J.D. Nicholas, and J.D. Bass (2004), Sound velocitymeasurements on laser-heated MgO and Al2O3, *Phys. Earth Planet. Inter., 143–144*, 575–586.

Sinogeikin, S. V., T. Katsura, and J.D. Bass (1998), Sound velocities and elastic properties of Fe-bearing wadsleyite and ringwoodite, *J. Geophys. Res.*, 103, 20,819–20,825.

Skinner, B. J. (1956), Physical properties of end-members of the garnet group, *Am. Mineral., 41*, 428–436.

Speziale, S. and T. S. Duffy (2002), Single-crystal elastic constants of fluorite (CaF_2) to 9.3 GPa, *Phys. Chem. Miner., 29*, 465–472.

Speziale, S., T. S. Duffy, and R. J. Angel (2004), Single-crystal elasticity of fayalite to 12 GPa, *J. Geophys. Res., 109*, B12, B12202, doi:10.1029/2004JB003162.

Stixrude, L., and C Lithgow-Bertelloni (2005), Mineralogy and elasticity of the oceanic upper mantle: Origin of the low velocity zone, J. Geophys. Res., in press.

Su, W-J., and A. M. Dziewonski (1997), Simultaneous inversion for 3D variations in shear and bulk velocity in the mantle, *Phys. Earth Planet. Inter., 100*, 135–156.

Sumino, Y., and O. Nishizawa (1978), Temperature variation of elastic constants of of pyrope-almandine garnets, *J. Phys. Earth, 26*, 239–252.

Sumino, Y., O. Nishizawa, T. Goto, I. Ohno, and M. Ozima (1977), Temperature variation of elastic constants of single-crystal forsterite between -190 and 400° C, *J. Phys. Earth, 25*, 377–392.

Suzuki, I., and O. L. Anderson (1983), Elasticity and thermal expansion ofa natural garnet up to 1,000 K, *J. Phys. Earth, 31*, 125–138.

van der Hilst, R.D., and H. Kárason (1999), Compositional heterogeneity in the bottom 100 kilometers of the Earth's mantle: toward a hybrid convection model, *Science, 283*, 1885–1888.

Vacher, P., A. Moquet, and C. Sotin (1998), Computation of seismic profiles from mineral physics: the importance of the non-olivine components for explaining the 660 depth discontinuity, *Phys. Earth. Planet. Inter., 196*, 275–298.

Wang, J., S. V. Sinogeikin, T. Inoue, and J.D. Bass (2003), Elastic properties of hydrous rongwoodite, *Am. Mineral., 88*, 1608–1611.

Watanabe, H. (1982), Thermochemical properties of synthetic high-pressure compounds relevant to the earth's mantle, in *High pressure Research in Geophysics*, edited by S. Akimoto and M. H. Manghnani, pp. 441–464, Center for Academic Publications, Tokyo, Japan.

Watt, J. P., G. F. Davies, and R. J. O'Connell (1976), The elastic properties of composite materials, *Rev. Geophys. Space Phys., 14*, 541–563.

Webb, S. and I. Jackson (1993), The pressure dependence of the elastic moduli of single –crystal orthopyroxene $(Mg_{0.8}Fe_{0.2})SiO_3$, *Eur. J. Mineral., 5*, 1111–1119.

Weidner, D. J., H. Wang, and J. Ito (1978), Elasticity of orthoenstatite, *Phys. Earth Planet. Inter., 17*, P7–P13.

Weidner D. J., H. Sawamoto, S. Sasaki, and M. Kumazawa (1984), Single-crystal elastic properties of the spinel phase of Mg2SiO4, *J. Geophys. Res., 89*, 7852–7860.

Xia, X., D. J. Weidner, and Y. Zhao (1998), Equation of state of brucite: Single-crystal Brillouin spectroscopy study and polycrystalline pressure-volume-temperature measurement, *Am. Mineral., 83*, 68–74.

Yeganeh-Haeri, A., D. J. Weidner, and E. Ito (1990), Elastic properties of the pyroxene-majorite solid solution series, *Geophys. Res. Lett., 17*, 2453–2456.

Yoneda, A., and M. Morioka (1992), Pressure derivatives of elastic constants of single crystal forsterite, in *High-pressure research: Application to Earth and planetary sciences*, edited by Y. Syono and M. H. Manghnani, pp. 207–214. Terra Scientific Company (TERRAPUB), Tokyo / American Geophysical Union, Washington, D.C.

Zha, C-S., T. S. Duffy, R. T. Downs, H-K. Mao, and R. J. Hemley (1996), Sound velocity and elasticity of single-crystal forsterite to 16 GPa, *J. Geophys. Res., 101*, 17535–17545.

Zha, C-S., T. S. Duffy, H-K. Mao, R. T. Downs, R. J. Hemley, and D. J. Weidner (1997), Single-crystal elasticity of β-Mg_2SiO_4 to the pressure of the 410 km seismic discontinuity in the Earth's mantle, *Earth and Planet. Sci. Lett., 147*, E9–E15.

Zha, C-S., T. S. Duffy, R. T. Downs, H-K. Mao, and R. J. Hemley (1998), Brillouin scattering and X-ray diffraction of San Carlos olivine: direct pressure determination to 32 GPa, *Earth Planet. Sci. Lett., 159*, 25–33.

Zha, C-S., H-K. Mao, and R. J. Hemley (2000), Elasticity of MgO and a primary pressure scale to 55 GPa, *Proc. Natl. Acad. Sci. USA, 97*, 13,494–13,499.

T. S. Duffy and F. Jiang, Department of Geosciences, Guyot Hall, Princeton University, Princeton, New Jersey 08544-1003, USA. (duffy@princeton.edu)

Sergio Speziale, Department of Earth and Planetary Science, 307 McCone Hall, University of California, Berkeley, California 94720-4767 USA.